Proiect cofinanțat din Fondul Social European prin Programul Operațional Sectorial Dezvoltarea Resurselor Umane 2007-2013
Investește în oameni!
Proiect InnoRESEARCH - POSDRU/159/1.5/S/132395
Burse doctorale și postdoctorale în sprijinul inovării și competitivității în cercetare

POLITEHNICA UNIVERSITY OF BUCHAREST
Faculty of Power Engineering
Department of Hydraulics, Hydraulic Machinery and Environmental Engineering

Senate Decision No. 183 from 14.12.2017

PhD THESIS

Correlation between a ship's geometric and functional parameters and channel navigation

Corelația între parametrii geometrici și funcționali ai unei nave și navigația în canale

Author: Eng. Petru Sergiu ŞERBAN
Coordinator: Prof. emeritus eng. Valeriu Nicolae PANAITESCU, PhD

EVALUATION BOARD OF THE PhD THESIS

President	Prof. eng. Adrian BADEA, PhD	from	Politehnica University of Bucharest
Coordinator	Prof. emeritus eng. Valeriu Nicolae PANAITESCU, PhD	from	Politehnica University of Bucharest
Scientific referees	Prof. eng. Beazit ALI, PhD	from	Naval Academy "Mircea cel Bătrân" of Constanța
Scientific referees	Prof. eng. Viorel ANDREI, PhD	from	"Dunărea de Jos" University of Galați
Scientific referees	Prof. eng. Carmen Anca SAFTA, PhD	from	Politehnica University of Bucharest

Bucharest

TABLE OF CONTENTS

KEY WORDS

canal, squat, ship, model, hull, channel, under keel clearance, towing tank, block coefficient of fineness, blockage factor, interaction, bank effect, depth, numerical simulation, turbulence model, CFD.

LIST OF ABBREVIATIONS AND NOTATIONS

Greek symbols

Symbol	Description	Dimensions
ε	Dissipation of turbulent kinetic energy	L^2T^{-3}
θ	Channel bank inclination angle	1
ν	Kinematic viscosity	L^2T^{-1}
ρ	Density	ML^{-3}
τ_w	Wall shear stress	$ML^{-1}T^{-2}$
ω	Specific dissipation of turbulent kinetic energy	T^{-1}
∇	Volume of displacement	L^3

Roman symbols

Symbol	Description	Dimensions
A_C	Canal/channel section area	L^2
A_N	Area of submerged amidships section	L^2
b	Ship breadth	L
B	Rectangular canal width at water surface	L
D	Ship construction height	L
e_{ch}	Distance from ship to the center of the canal	L
F_B	Width of influence	L
F_D	Depth of influence	L
F_Z	Buoyancy total force	MLT^{-2}
h	Water depth	L
h_T	Depth of dredged underwater trench	L
k	Kinetic energy of turbulence	L^2T^{-2}
L_{pp}	Length between perpendiculars	L
n	Canal bank slope	1
p	Pressure	$ML^{-1}T^{-2}$
S_m	Medium squat	L
$S_{\max}$	Maximum squat	L
S_{pp}	Stern squat	L
S_{pv}	Bow squat	L
T	Draft	L
u_*	Friction speed	LT^{-1}
U	Fluid speed	LT^{-1}
ukc	Under keel clearance	L
V_K	Ship speed in knots	LT^{-1}
V_N	Ship speed in m/s	LT^{-1}
W_0	Trapezoidal canal width at water surface	L
W	Canal width at bottom	L
W_{eff}	Effective width	L
y_{ch}	Distance between ship's centerline and canal bank	L

Dimensionless numbers

Symbol	Description	Definition
C_B	Block coefficient of fineness	$C_B = \dfrac{\nabla}{L \cdot b \cdot T}$
h/T	Dimensionless depth ratio	*
S	Blockage factor	$S = \dfrac{A_N}{A_C}$
y^+	Dimensionless distance to wall	1

ACKNOWLEDGMENT

I would like to express my sincere thanks to the coordinator, *Prof. emeritus eng. Valeriu Nicolae PANAITESCU, PhD*, for the coordination with wisdom and scientific rigor of the researches. The professor has been a model for me in these five years, always giving me the encouragement and motivation needed in less good times. I wish him much health, to keep his spirit young for many years now and I assure him of all my gratitude.

I would also like to thank all the members of the doctoral committee who unconditionally supported me in the elaboration of the thesis:

Mrs. *Prof. eng. Carmen Anca Safta, PhD*, for the critical, intransigent and constructive spirit that helped the development of the thesis;

Mr. *Prof. eng. Beazit Ali, PhD*, for the useful advice given and the solicitude shown every time;

Mr. *Prof. eng. Viorel Andrei, PhD*, for the patience with which he analyzed the present paper.

At the same time, I would like to thank the collective of the Naval Academy "Mircea cel Bătrân" in Constanţa for the understanding given over time:

Mr. *Captain (N) Assoc. prof. eng. Alecu Toma, PhD*, the person who guided me to the field of research and was always close to me;

Mr. *Assoc. prof. eng. Marian Ristea, PhD*, for useful advice and support in numerical simulations;

Mr. *Rear-Admiral (R), Prof. eng. Vergil Chiţac, PhD*, for the trust and facilitation of my participation in the training voyage with "MIRCEA" sailing ship;

Mr. *Lieutenant Commander (N) Assoc. prof. eng. Sergiu Lupu, PhD*, Director of the department which I am part of, for his support in solving organizational problems in the department.

I would not have succeeded in my approach without the family being close to me. I thank my parents, my father *Gheorghe Şerban* and my mother *Mioara Şerban*, for the education, the moral and material support they have given, and my wife *Maria Raluca Şerban*, for her understanding and the support she have given over the years, with the promise to recompense for all the sacrifices made.

Thousands of thanks to all those who supported me and whom, unintentionally, I forgot.

INTRODUCTION

1. THE TOPICALITY AND OPPORTUNITY OF THE DOCTORAL THESIS

Over the last decade, there has been observed a steady increase in ship size, particularly oil tankers, container carriers, RO - RO[1] ships or LNG carriers. On the other hand, the dimensions of the canals or rivers and the ports frequented by these ships types usually do not increase at the same pace. Consequently, the behavior of the vessels in these areas is largely influenced by the restrictive conditions of the navigation routes.

A moving vessel continuously displaces and accelerates a significant amount of water, which, according to *Bernoulli*'s principle, leads to a drop in pressure around the ship. The latter produces a vertical displacement characterized by a sinking of the ship at the forward and aft perpendiculars[2], or, alternatively, a medium immersion and a trim. This phenomenon is called *squat*. The phenomenon is of great interest for the current evolution of the shipbuilding industry and science, being debated in international conferences and studied in various universities and specialized institutes in the European Union and other countries, where extensive research is carried out on the improvement of study methods.

2. THESIS OBJECTIVES

Taking into consideration the necessity of accurate estimation of the squat phenomenon and the actuality of the subject, the PhD thesis entitled *"Correlation between a ship's geometric and functional parameters and channel navigation"* – initially, proposes a theoretical approach to the production of this phenomenon with consequences on safe navigation in shallow water conditions, focusing on numerical analysis and case studies of the squat for different vessel types and channel configurations, and ultimately

[1] roll on – roll off – type of seagoing vessel specialized for the transport of road vehicles, container trailers, tracked vehicles, buses, etc.

[2] forward perpendicular – perpendicular to the base plane which is lowered from the point of intersection of the forward extremity with the full-load line;aft perpendicular - perpendicular to the base plane passing through the rudder shaft

assessing squat production on board training ship "MIRCEA" through experimental research and CFD[3] numerical simulations.

Starting from this goal, the operational objectives of the thesis can be defined as follows:

- assessing the current state of research on the squat phenomenon and identifying the most widely used waterways in maritime transport;
- the theoretical study of the squat and the determining factors, as well as a comprehensive analysis of the computational relations existing in the literature;
- conducting a simulation study on the production of squat on military ships and the danger of their grounding through Sulina Canal;
- numerical assessment of squat produced on different categories of merchant vessels to navigate through two types of channels;
- carrying out case studies on ship-to-ship and ship-to-shore interaction in the Suez Canal;
- analysis of the opportunity of squat on board training ship "MIRCEA" through experimental research;
- numerical simulation of the hydrodynamic parameters of the training ship "MIRCEA" hull in different depth domains using ANSYS;
- assessment of the squat determined using the CFD method in comparison with empirical computational relations existing in the literature.

CHAPTER 1
NAVIGATION CHANNELS USED IN MARITIME TRANSPORT AND STATE OF EXPERIMENTAL RESEARCH ON SHIP SQUAT

1.1. CANAL NAVIGATION

A navigable channel is a narrow transit route connecting two significantly larger waters. In the most common cases it refers to a stretch of water along two massive areas, but it can also be referred to a waterway that is already in a water-covered area, but which is not navigable, but due to its work, can be turned into a safe navigation route.

Navigation through canals, narrow passes and generally difficult passes involves some preliminary tasks of the master and crew.

Unless otherwise specified in the transit instructions, navigation shall be as close to the right as possible, with ships crossing the port side. The ship, which reaches another ship, overtakes her in port side, with the starboard side.

1.2. NAVIGATION CANALS USED IN MARITIME TRANSPORT

1.2.1. Danube – Black Sea Canal

The Danube - Black Sea Canal is a navigable canal that connects the Cernavodă port on the Danube and the Constanța and Midia ports of the Black Sea, shortening the road to the port of Constanța with about 400 km. The canal, with a total length of 95.6 km, consists of the main branch and the north branch, known as the Poarta Albă – Midia – Năvodari Canal, 31.2 km long.

1.2.2. Suez Canal

The Suez Canal, situated west of the Sinai Peninsula, is a 193.3 km long, 313 m wide channel, at its narrowest point, and 24 m deep. With a trapezoidal section, the canal width at 11 m depth is 205 – 225 m. It is located in Egypt, between Port Said (*Būr Sa'īd*) from the Mediterranean Sea and Suez (*al-Suways*) from the Red Sea.

1.2.3. Panama Canal

The Panama Canal crosses the Isthmus of Panama in Central America, linking the Pacific Ocean and the Atlantic Ocean. The channel has had a tremendous impact on navigation because ships no longer have to pass through South America at Cape Horn, shortening the distance between New York and San Francisco from 22,500 km to 9,500 km. Each year more than 14,000 ships pass through the canal, carrying more than 20,378 million tons of freight.

[3] Computational Fluid Dynamics

1.2.4. Kiel Canal

The Kiel Channel (Nord – Ostsee – Kanal) is located in northern Germany, uniting the Baltic Sea with the North Sea, shortening with 400 km the water link between Hamburg and Kiel. The canal measures 98.7 km in length, has a maximum width of 162 m at water surface and 90 m at the bottom, with a water depth of 11 m.

1.2.5. Corinth Canal

The Corinth Canal connects the Gulf of Corinth and the Saronic Gulf in the Aegean Sea. It passes through the narrowest part of the Isthmus of Corinth and separates the Peloponnese Peninsula from the rest of Greece. The channel consists of a single 8 m deep waterway, dredged at the sea level. It has a total length of 6343 m, a width of 21.3 m at its base and 24.6 m at sea level. The channel's rock banks rise to a maximum height of 79 m above sea level and are almost vertical. The maximum crossing height below the bridges crossing the channel is 52 m.

1.3. STATE OF THE ART ON EXPERIMANTAL RESEARCHES CARRIED ON SHIP SQUAT

Scientific research on squat was begun by *Constantine* (1960), who studied squat behavior for subcritical, critical and supercritical speeds. More practical methods based on experimental research are presented by *Barrass* (1979), who also proposed an equivalent width, taking into account the width of the canal. General approaches are also presented by *Dumas* (1982), *Millard* (1990), PIANC[4] (1997) and *Blaauw* and *Van der Knaap* (1983). *Jiang* and *Henn* (2003) present a valid numerical method for subcritical and supercritical speeds. Squat in muddy areas was investigated by *Sellmeijer* and *van Oortmerssen* (1983), *Doctors et al*. (1996) and most recently by *Delefortrie et al*. (2010).

1.3.1. Types of models tested

Between 2001 and 2004, at Ghent University, Belgium, it was studied the phenomenon of squat in muddy areas on three ship models. The research was carried out in a towing tank of 88 m × 7 m × 0.5 m. A study published in 2013 shows the interaction between two types of vessels in a canal, passing one next to each other. Another study on scale models has led to the squat of a ship with a block coefficient of fineness[5] of 0.6, located in a shallow water canal.

In 2013, for squat measurements, a 1:45.71 scale KVLCC[6] tanker was used in a variable depth basin. The towing tank in which the tests were conducted measures 220 m long, 9 m wide and 3.8 m deep. The depth of water (*h*) in the towing tank was varied by means of a false floor, thus obtaining different *h/T* depth ratio values.

Most theoretical, numerical and experimental studies on the squat examination and prediction take into account one parameter, ship's speed, and it is based on the premise that the ship is moving straight at the center of the canal. In reality, a ship is subject to wind and current effects, may accelerate or decelerate, and must change its course. In a two-way canal, the trajectory of the ship is eccentric and its hydrodynamics is influenced by interaction with other vessels during overtaking or passing maneuvers [14].

1.3.2. Methods of measurement, similarity criteria

In order to study the behavior of vessels using models, the criteria of similarity must be established: geometric, cinematic and dynamic. For kinematic and dynamic similarity, the Froude, Strouhal, Webber and Reynolds numbers must be the same for both the ship and the model. To reduce the risk of large errors due to the inequality of the Reynolds and Webber numbers, the ship model must be large enough. In reality, errors occur when the results obtained on the model are extrapolated to the ship, a phenomenon known as the scale effect. This is due to the inequality of other dimensionless numbers of the model and the ship.

1.3.3. Towing tanks

The towing tank used by Ghent University, Belgium, has the following dimensions: 87.5 m long, of which 68 m are useful for experiments, 7 m wide and 0.5 m water deep. The dimensions of the tank are modest but sufficient to perform maneuver and sea-keeping tests on models with lengths between 3.5 and 4.5 m, at speeds up to 1.2 m/s (fig 1.1). Ship models drafts vary between 0.1 and 0.2 m. The basin is also equipped with a wave generator to study ships interaction or bank effect.

[4] Permanent International Association of Navigation Congresses

[5] block coefficient of fineness – dimensionless, subunit size representing the ratio between the hull volume and the volume of a parallelepiped in which the hull engraves

[6] KRISO (Korea Research Institute of Ships and Ocean Engineering) Very Large Crude Carrier

Fig. 1.1. The track drawbar system of the towing tank [20]

At the Faculty of Naval Architecture from "Dunărea de Jos" University in Galați there is also a towing tank measuring 45 m × 4 m × 3 m, equipped with an automatic towing system. Tests on ship models, up to 4 m in length and a maximum mass of 200 kg, can be executed at constant speeds of 4 m/s.

CHAPTER 2
THEORETICAL CONSIDERATIONS AND CASE STUDIES ON MARITIME SHIPS SQUAT

2.1. SHIP SQUAT

Squat is a drop in under keel[7] clearance, caused by the moving of the hull through the volume of surrounding water. Compared to the ship's neutral position, the hull enters more into the water and at the same time changes its trim[8].

When a ship advances through the water, it pushes the water from its bow. In order for not to be an "empty" water, this volume must return along the hull beneath the ship's body. Flow rates below the ship increase their speed, causing a drop in pressure that leads to a downward movement of the ship. In shallow water and/or narrow water, the flow rate of water particles increases, resulting in a pressure drop, according to *Bernoulli*'s law. With this vertical downward movement, the ship will change its trim, leaning towards the bow or stern. The total drop in the bow or stern of the under keel clearance relative to the depth when the ship is on even keel is called **squat** (fig. 2.1).

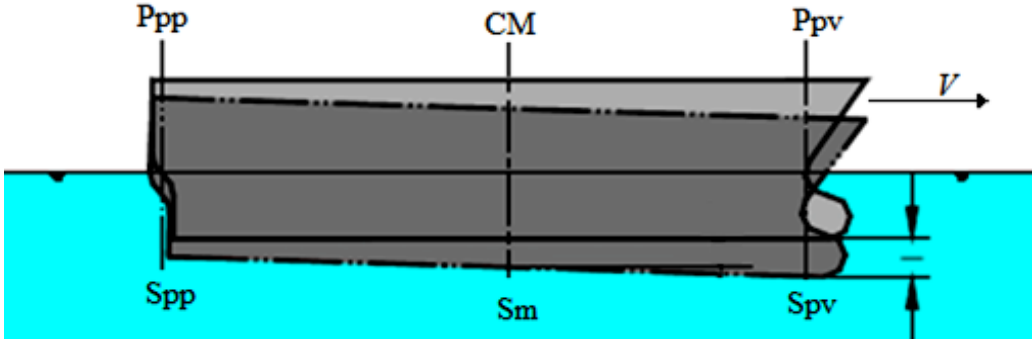

Fig. 2.1. Ship squat (S_{pv} – bow squat, S_m – medium squat, S_{pp} – stern squat) [6]

For ships with full forms such as oil tanks or cargo ships, the grounding due to squat occurs at the bow, and for fine form ships such as passenger ships or container vessels, grounding usually occurs at the stern.

[7] keel – the main element in the longitudinal structure of the ship, consisting of a metal beam or a continuous thick sheet of steel from bow to stern in the diametrical plane at the bottom of the ship

[8] trim – a naval term indicating the longitudinal inclination of a ship due to the uneven distribution of the load or ballast

2.2. DETERMINANT FACTORS OF SQUAT

2.2.1. Ship characteristics

The main parameters of the vessel that influence the squat are the draft T, the shape of the hull, represented by the block coefficient of fineness C_B, the speed in m/s V_N or in knots V_K, the length between perpendiculars L_{pp} and the breadth b.

The block coefficient of fineness is a measure of the *fineness* of the ship's shape relative to an equivalent parallelepipedic volume of the same dimensions. The values of the block coefficient of fineness usually vary between 0.45 for fine-form vessels and 0.85 for full-form vessels.

The most important parameter is V_K, which is the speed of the ship through water, so the direction and speed of water currents and tidal currents must be taken into account. Usually squat varies with the square of speed. In other words, if the speed is halved, the squat will become four times smaller [4].

There are also two parameters calculated on the ship's dimensions. The volume of water displaced by the ship is defined as the product of the block coefficient of fineness, the length between perpendicular, breadth and draft,

$$\nabla = C_B \cdot L_{pp} \cdot b \cdot T \quad [\mathrm{m}^3]. \tag{2.1}$$

The area of the immersed amidships surface is A_N and is defined as

$$A_N = 0.98 \cdot b \cdot T \quad [\mathrm{m}^2]. \tag{2.2}$$

2.2.2. Canals configuration

The main types of configurations of waterways are open or unrestricted, restricted (bottom dredged) and canal.

Unrestricted waterways (fig. 2.2.a) are relatively large stretches of water without side restrictions but with shallow waters, and are usually encountered at channel entrances. The second type of channel (fig. 2.2.b) shows at its bottom a dredged underwater hat, h_T, which does not protrude to the surface of the water. The channel is defined by the total depth h and the width at the bottom of the channel, W. The last type of configuration is the canal (fig. 2.2.c). This characterizes the canals with consolidated banks, which may or may not be exposed to tidal fluctuations. The canal configuration is characterized by: the width at the bottom W, the depth h and the slope of the side wall or bank n, where n = 1/tg θ [6].

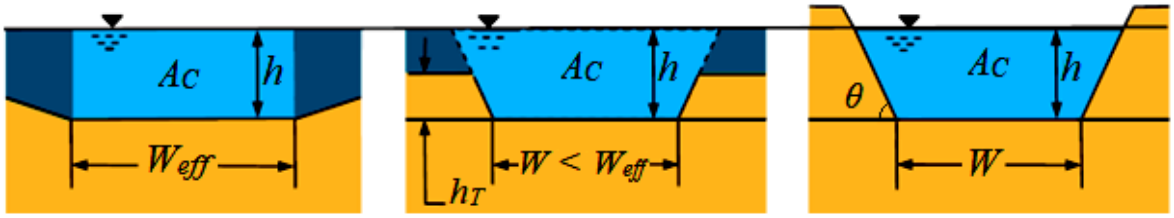

(a) (b) (c)

Fig. 2.2. Schematic representation of the cross section types of waterways [8]

2.2.3. The combination of ship and canal characteristics

Several dimensionless parameters are required to be used in squat calculation formulas, the most important being the Froude number of depth Fr_h, which is a measure of the ship's resistance to advancing in shallow waters.

The second non-dimensional parameter is the blockage factor, S and represents the ratio between the ship's immersed amidships section, A_N and the cross section of the canal or the waterway, A_C (fig. 2.3). It is defined as

$$S = \frac{A_N}{A_C} = \frac{0.98 \cdot b \cdot T}{B \cdot h}. \tag{2.3}$$

Blockage factor values are typically between 0.03 and 0.25 or greater for restricted (bottom drag) channels or 0.10 or less for unrestricted waterways [4].

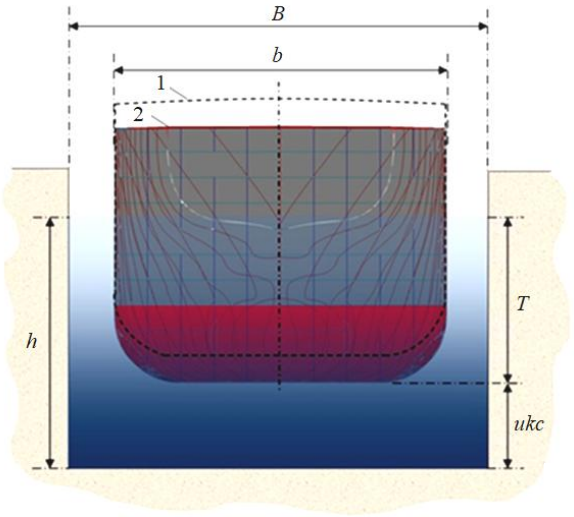

Fig. 2.3. Ship in a canal
(*B* – canal width, *h* – water depth, *b* – ship breadth, *T* – ship draft, *ukc* – under keel clearance;
1 – ship's static position, 2 – ship's position at V_K speed)

2.2.4. Width of influence

If a ship is in open water conditions, there are two artificial limits on the starboard and port side, parallel to the ship's centerline, outside of which an obstacle can not bring any change in vessel speed, resistance or squat. This artificial limit is known as the *width of influence*, denoted by F_B.

2.2.5. Depth of influence

There is also a *depth of influence*, denoted by F_D, which defines an artificial depth limit. If the depth of water *h* is greater than the depth of influence, the ship is not influenced by the bottom of the waterway or canal. Otherwise, the presence of the bottom will cause changes in the ship's hydrodynamics and may influence squat.

It is said that a ship is in "*open water*" conditions when it sails in shallow waters but without side restrictions. A vessel found in shallow waters and having side restrictions is considered to be in narrow canal or "*restricted waters*".

2.2.6. Effects of limited depth and canal navigation on ship's resistance

The limited depth influences both the viscosity resistance and the wave resistance. Thus, in the boundary layer, appear areas of local speed increase, which increase the shear stresses and the frictional resistance. There is also an accentuation of pressure drops, leading to the separation of the boundary layer and the increase in shape resistance.

2.3. MAXIMUM SQUAT CALCULATION

The squat calculation formula was designed to meet an estimate of the maximum squat for ships sailing both in straits, canals or narrow passageways and under open or unrestricted canal conditions. The formula developed by *Barrass* is among the most simple and easy to use for all types of channel configurations. Based on his research in the years 1979, 1981 and 2004, the maximum squat formula is determined by the block coefficient of fineness C_B, the blockage factor *S* and the ship's speed in knots, V_K.

Maximum squat $S_{\max}$ is equal to

$$S_{\max} = \frac{C_B \cdot S^{0.81} \cdot V_K{}^{2.08}}{20} \text{ [m].} \tag{2.4}$$

The main factor is the ship's speed. In-depth research has shown that squat varies with speed at power of 2.08. In this context, V_K is the ship's speed through water; so the effect of current or tide must be taken into account.

The value of the block coefficient of fineness C_B determines whether the maximum squat occurs at the bow or stern in the case of even keel vessel. Full-formed vessels with $C_B > 0.700$ tend to have squat at the bow, while fine-formed vessels with $C_B < 0.700$ tend to have it at the stern. Vessels with $C_B = 0.700$ have a full-length immersion equal to the maximum squat value [3].

Figure 2.4 shows the maximum squat for commercial ships with a block coefficient of fineness between 0.500 and 0.900, both in open water and confined channels. In order to use the diagram, three

values must be known: block coefficient of fineness, ship speed and navigation conditions (open water, confined river/canal conditions). After knowing this information and a quick grading of the graph, an approximation of the squat will result. If the under keel clearance, after considering the increase of the draft due to squat, is not high enough for safe navigation, then the speed of the ship needs to be reduced [3].

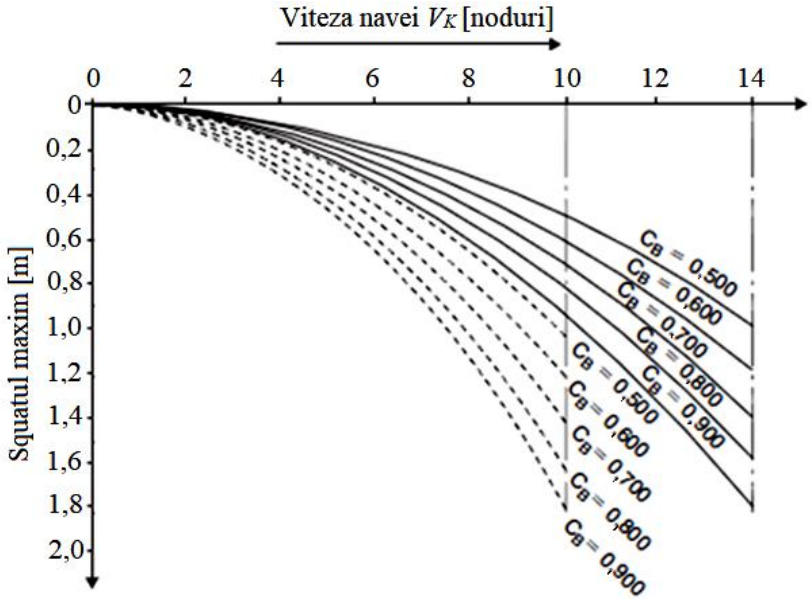

Fig. 2.4. Maximum ship squats in confined channels and in open water conditions (----- denotes ship is in a confined channel, where S = 0.100 – 0.266; —— denotes ship is in open water, where h/T = 1.10 – 1.40) (processing after *Barrass* [3])

2.4. EMPIRICAL RELATIONS OF SHIP SQUAT

The most representative squat calculation formulas are presented below. Some of these offer good results, being often validated; others are based on more recent research. Table 2.1 shows the characteristics of the channels for which these formulas can be applied and the restrictive parameters according to their individual test conditions.

Table 2.1. Restrictive parameter values of squat calculation formulas (processing after *Briggs* [6])

	Waterway type*			**Restriction type**				
Formula	*U*	*R*	*C*	C_B	*b/T*	*h/T*	*L/b*	*L/T*
Barrass	X	X	X	0.5 – 0.9		1.1 – 1.5		
Eryuzlu and *Hausser*	X			≥ 0.8		1.08 – 2.75		
Eryuzlu ș.a.	X	X		≥ 0.8	2.4 – 2.9	1.1 – 2.5	6.7 – 6.8	
Huuska	X	X	X	0.6 ≥ 0.8	2.19 – 3.5	1.1 – 2.0	5.5 – 8.5	16.1 – 20.2
ICORELS[9]	X							
Yoshimura	X	X	X	0.55 – 0.8	2.5 – 5.5	≥ 1.2	3.7 – 6.0	
Millward	X			0.44 – 0.83				
Romisch	X	X	X		2.6	1.19 – 2.25	8.7	22.9
Soukhomel and *Zass*	X					1.2 – 1.5	3.5 – 9.0	

* U – unrestricted, R – restricted, C – canal

All of these formulas offer predictions of bow squat, S_{pv}, for all channel types, except for the *Romisch* formula, which gives prediction of both bow and stern squat. *Barrass*'s formula calculates stern squat for unrestricted, restricted channels and canals, but it depends on the value of block coefficient of fineness, C_B. Each formula has certain constraints that must be satisfied before it is applied. If these formulas are used in conditions other than those for which they have been developed, particular attention should be paid.

[9] International Commission for the Reception of Large Ships

2.5. SHIP SQUAT FOR SHIPS WITH STATIC TRIM

If vessels are assumed to on even keel, for a certain speed value and block coefficient of fineness, then the maximum squat can be calculated, which occurs at the aft, the bow, or the full length of the ship.

If, instead, ships are already assumed to have a static trim, when moving, the maximum squat is determined by the trim. Tests on models as well as ship showed the following:

- if a ship is trimmed by the stern when static, then it has the maximum squat at the stern when moving with forward speed;
- if a ship is trimmed by the head when static, then it has the maximum squat at the bow when moving with forward speed.

2.6. CASE STUDY ON SHIP SQUAT IN SULINA CANAL USING THE NTPRO 5000 NAVIGATION SIMULATOR

This subchapter presents a case study on the squat phenomenon by simulating navigation at the entrance to the Sulina Canal of four Navy ships from the NTPRO 5000 simulator. The purpose of these simulations was to see what types of military ships can navigate through the Sulina Canal and which is the maximum allowed speed, without grounding due to squat. So far, no simulations have been carried out on the squat phenomenon on military ships in the Sulina Canal.

2.6.1. Simulated trials

The ships used for the simulations were two frigates, a patrol vessel (OPV[10]) and a multirole vessel (MSS[11]), which have similar characteristics to the vessels of the Romanian Navy. Their technical characteristics are presented in table 2.2.

Table 2.2. Military ship's characteristics

Characteristics	U.M.	Frigate 1	Frigate 2	MSS	OPV
Displacement	[t]	3664	3600	2250	1706
Length	[m]	130.5	118	73	85
Breadth	[m]	14.6	14,8	13,8	14
Bow/ stern draft	[m]	3.92/ 4.64	4.37/ 4.37	4.3/ 4.3	3.56/ 3.63
Maximum speed	[knots]	32.4	26.6	13.6	22.5

The simulations begin with the vessels at the entrance to the canal, in the middle of it and navigate upstream at constant speed (fig. 2.5). During the tests, the ship's passing was observed for a distance of one nautical mile[12], after which the exercise was stopped.

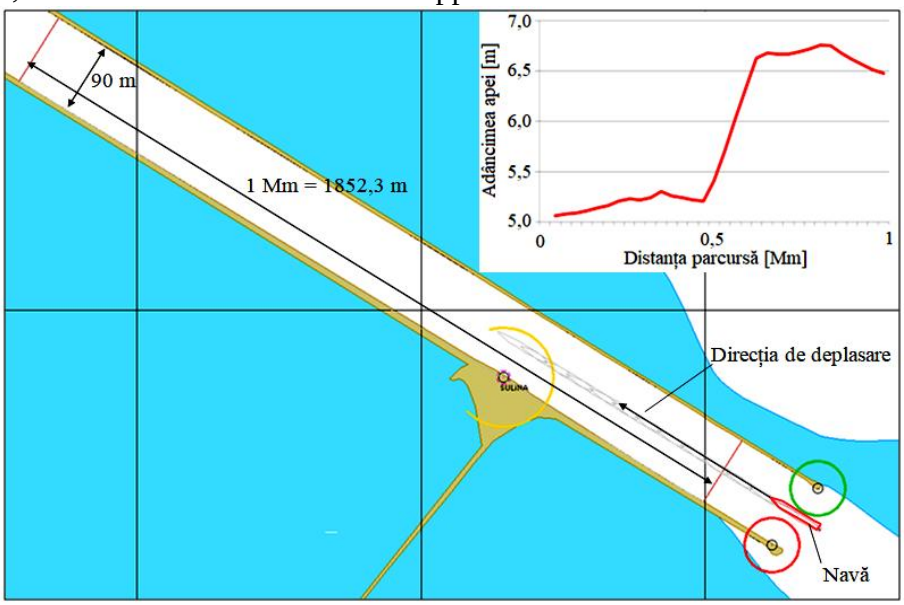

Fig. 2.5. Entrance of Sulina Canal. Water depth variation [TRANSAS Navi-Sailor 4000]

[10] Offshore patrol vessel
[11] Multirole support ship
[12] nautical mile – unit of measure of distance, used in naval and aviation, equal to 1852.3 m

In the NTPRO 5000 navigation simulator, the water depth in the chosen area ranged from 5 to 7 m, and considering the ships' drafts and the canal width of 90 m, it can be said that restricted shallow water conditions are met. So when ships pass through these areas they are affected by the squat phenomenon and suffer an increase in draft. The initial speed V_K used for the tests started in each case from 4 knots (about 2.06 m/s), being constantly increased until the vessels grounded due to squat.

2.6.2. Results interpretation

By analyzing the results of the simulations, it has been shown the maximum speed of each ship that allows navigation through the Sulina Canal without grounding and how squat varies when the ships are in motion.

❖ **Frigate 1**

During the tests, the speed of the vessel was increased consecutively from 4 to 8 and 12 knots. The draft is constant during the passage through the channel; at 4 knots, the draft of the ship at the bow does not change, but at the stern, it slightly increases due to the squat effect, from 4,6 m, at static conditions, to 4,7 m. At this speed the squat is very small, 0.1 m. After the first test of Frigate 1, the exercise was resumed under the same conditions, but at 8 knots. In this case, the ship's draft increases due to the squat effect, reaching a maximum of 3.96 m at the bow and 4.85 m at the aft. When the water becomes deeper, the squat becomes smaller and the draft decreases. The third test was performed at 12 knots. At this speed, the draft at the bow is 0.01 m higher than in the previous one, while at the aft it increases to a maximum of 5.01 m. Therefore, Frigate 1 cannot navigate the channel at the speed 12 knots, the maximum speed being 8 knots, and the safety speed, 4 knots.

❖ **Frigate 2**

In the tests performed with Frigate 2, the speed was increased consecutively from 4 knots to 8, 12 and 14 knots. At 4 knots, the squat effect produces a slight increase in draft, from 4.37 m to the bow under static conditions at 4,4 m and 4,44 m at the stern. In this case, the under keel clearance allows the frigate to navigate through the channel.

For 8 and 12 knots, the drafts and under keel clearance trends are similar to that of the Frigate 1. The trial at 14 knots showed that the bow draft slightly increased from 4.31 m to 4.45 m, while the stern draft dropped from 4.94 m to 4.92 m, when the ship reaches the one nautical mile limit. The under keel clearance is 0.78 m at the bow and 0.08 m at the aft, which causes the ship to ground at speeds greater than 14 knots.

❖ **Multirole support ship**

For this ship the tested speeds were 4 and 8 knots, because at higher speeds the ship grounds, although larger vessels (Frigate 1 and 2) can navigate at speeds of up to 12 knots. This can be explained by the value of the coefficient block of fineness, C_B = 0.507, higher than the other vessels and the value of the blockage factor S = 0.130, which produces a larger squat than the existing under keel clearance. The drafts and under keel clearance trends are similar to that of Frigates 1 and 2, but also the speed difference is similar, with slight variations at 8 knots.

❖ **Offshore patrol vessel**

In this case, the speeds used were 4, 8, 12, 16 and 20 knots. In the first two trials (4 and 8 knots) there were no major changes in the trend of draft and under keel clearance compared to the other studied vessels. At 12 knots, however, the draft increases when the water becomes deeper, from 3.59 m to 3.64 m, while the aft draft decreases from 3.98 m to 3.83 m. The under keel clearance remains positive, having a minimum stern value of 0.84 m, which makes it possible to navigate the canal. At 16 knot speed, the draft and under keel clearance is similar to that of 12 knots, the stern draft having a maximum value of 4.21 m. At 20 knots, the ship trims even more by the stern, with small variations from previous tests; at the bow between 3.27 m and 3.38 m and a stern between 4.1 m and 4.23 m. The under keel clearance ranges from 1.67 m to 3.87 m at the bow and from 0.57 m to 3.15 m at the stern. At this speed, the stability and maneuverability of the ship are greatly affected by the waves reflected by the canal's banks, which in turn are generated by the large waves produced by the ship.

CHAPTER 3
ANALYSIS OF SQUAT AND UNDER KEEL CLEARANCE FOR VARIOUS SHIP TYPES

3.1. CALCULATION OF SQUAT AND UNDER KEEL CLEARANCE

The problem of squat and under keel clearance determination is particularly important for ships, especially in shallow waters conditions or in confined channels. In order to see how the squat of different types of ships varies according to the actual speeds allowed for channel navigation, calculations were made to determine it.

First of all, it is necessary to know the main dimensions of the different vessels used today in modern navigation. The most representative categories of ships in the shipbuilding industry were selected, and for each category, the average dimensions of the vessels, such as the length between perpendiculars, breadth, draft, block coefficient of fineness or cruise speed, were selected, the results being presented in table 3.1.

Table 3.1. The average dimensions of different ship types [4]

Ship type	L_{pp} [m]	b [m]	T [m]	C_B	F_B [m]	F_D [m]	V_K [knots]
ULCC[13]	350	65	23	0.850	525.2	126.1	14.5
VLCC[14]	318	60	20	0.825	497.4	114	15.5
Oil tanker	212.5	32.5	12	0.800	276.6	71.16	15.5
Bulk carrier	212.5	34.4	12.4	0.775	300.7	76.6	14.5
General cargo ship	125	20	7.8	0.700	190.6	55.1	14.5
Passenger liner	230	30	7.6	0.625	315	62.2	25
Container ship	250	37.5	11.4	0.575	422.6	104	23
RO – RO vessels	179.5	31.3	7.3	0.560	306.7	68.9	21
Tug	36.5	12.5	5.5	0.500	158.6	60.1	10

Two types of theoretical canals were chosen for this study, but with dimensions close to those of actual canals. The first one has a rectangular cross section, width B = 123 m and depth h = 24 m (fig. 3.1). The second type of channel has a trapezoidal cross section, similar to the shape of Suez Canal section, having the water surface width, W_0 = 313 m, width at the bottom, W = 121 m and depth, h = 24 m (fig. 3.2).

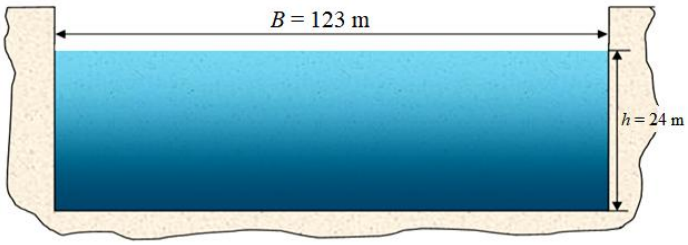

Fig. 3.1. Rectangular canal – cross section

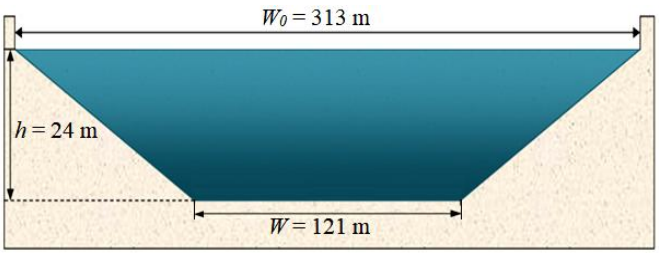

Fig. 3.2. Trapezoidal canal – cross section

Lastly, the speeds that were taken into account when determining the squat were established. For this squat analysis, the speeds of 6, 8, 10 and 12 knots (about 3, 4, 5 and 6 m/s respectively) were considered.

To determine the maximum squat S_{max} it was chosen *Barrass*'s formula (2.4) because it is among the most simple, easy to apply and valid for many types of ships and channel configurations. The blockage factor S was calculated with the relation (2.3) and the results obtained together with the value of immersed amidships section areas of the vessels were listed in table 3.2.

Considering the rectangular section canal and the aforesaid speeds for the selected vessel types, the maximum squat and under keel clearance (*ukc*) values were obtained, the last being determined with relationship

$$ukc = h - T - S_{max} \quad [\text{m}]. \tag{3.1}$$

[13] Ultra Large Crude Carrier
[14] Very Large Crude Carrier

Table 3.2. Blockage factors for the two types of canals

Ship type	b [m]	T [m]	A_N [m^2]	S_1	S_2
ULCC	65	23	1465.1	0.496	0.281
VLCC	60	20	1176	0.398	0.226
Oil tanker	32.5	12	382.2	0.129	0.073
Bulk carrier	34.4	12.4	418	0.142	0.080
General cargo ship	20	7.8	152.9	0.052	0.029
Passenger liner	30	7.6	223.4	0.076	0.043
Container ship	37.5	11.4	418.9	0.142	0.080
RO – RO vessels	31.3	7.3	223.9	0.076	0.043
Tug	12.5	5.5	67.4	0.023	0.013

Analyzing all the results, it is concluded that a ULCC vessel can not navigate on a rectangular canal of specified dimensions, regardless of its speed, and a reduction in speed below 6 knots, to obtain a lower squat and therefore a positive under keel clearance, leads to the decreasing of ship's maneuverability. VLCC vessels can transit such a channel up to 8 knots. Above this speed, the under keel clearance is very low and does not allow sailing safely. Squat for other ship types falls within normal limits, and the keel clearance is sufficient even at 12 knots.

In the next step, calculations were made for the same types of ships, the same speeds, but for the trapezoidal canal. The analysis of the results shows that even on the trapezoidal canal the ULCC can not navigate without grounding. Unlike the rectangular canal that allowed VLCC ships to navigate at a maximum speed of 8 knots, the trapezoidal canal offers the ability to navigate these ships at speeds of up to 12 knots.

In figures 3.3 and 3.4 it can be noticed that at all ship types squat increases with speed. The highest increase is in ULCC (C_B = 0.850) and VLCC (C_B = 0.800). At the opposite end, tugs (C_B = 0.500) have small variations of squat from one speed to another.

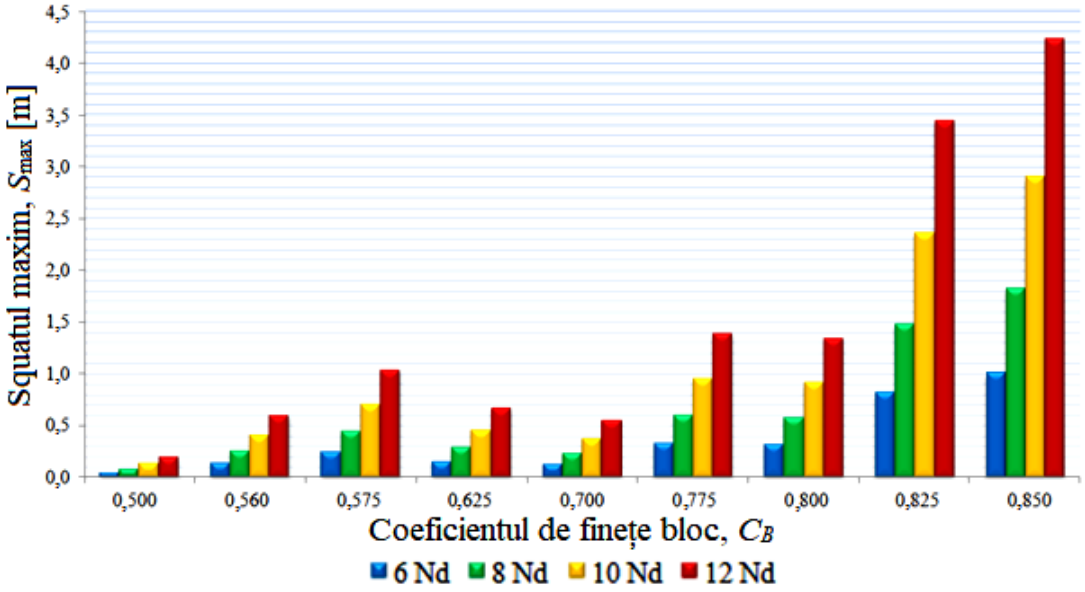

Fig. 3.3. Ship squat at considered speeds in the rectangular canal for different values of the block coefficient of fineness

Changing the cross section of the canal from the rectangular to the trapezoidal one it shows that the maximum squat values decrease by 37 %. Therefore, a wider channel is suitable for VLCC ships, while the rest of the considered ships do not depend on the shape of the cross section of the channel, which can navigate with all the considered speeds. Unlike these, ULCC-type ships do not meet the conditions of a sufficient under keel clearance to allow navigation, in most of the cases the ship grounds.

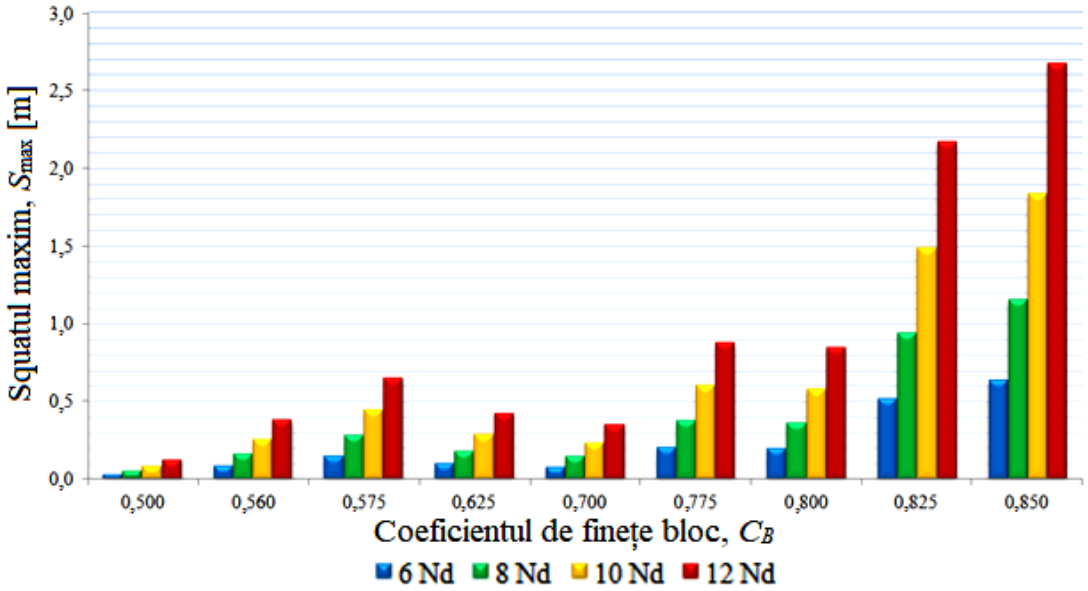

Fig. 3.4. Ship squat at considered speeds in the trapezoidal canal for different values of the block coefficient of fineness

3.2. CALCULATION OF SQUAT FOR A GENERAL CARGO SHIP IN VARIOUS TRAPEZOIDAL SECTION CANALS

3.2.1. Designing the ship in Autoship software

Autoship developed by Autoship Systems Corporation is a marine engineering software that provides cutting-edge software solutions for two major categories of marine industries: design and shipbuilding industry and shipping industry.

Following the study of the specialized bibliography and the dimensions of the current ships, it was chosen to model a general cargo ship with the dimensions shown in table 3.3.

Table 3.3. Main characteristics of the general cargo ship

Characteristics	Dimension	U.M.
Maximum length L	128	[m]
Breadth b	20.5	[m]
Draft T	6.5	[m]
Construction height D	15.5	[m]
Block coefficient of fineness C_B	0.700	–

The final shape of the ship following the modeling steps is shown in figure 3.5. Autoship offers the possibility of viewing the ship in all three planes, but also three-dimensional, with the option of rotating the ship's body in any direction.

The geometry of the vessel is concretized by lines plan obtained by dividing the ship with planes parallel to the main planes and overlapping the resulting curves. This is useful in making the calculations necessary for the design of the ship and during its operation; for example, at docking or body repairs, when it is necessary to detail the shape of the ship in certain areas.

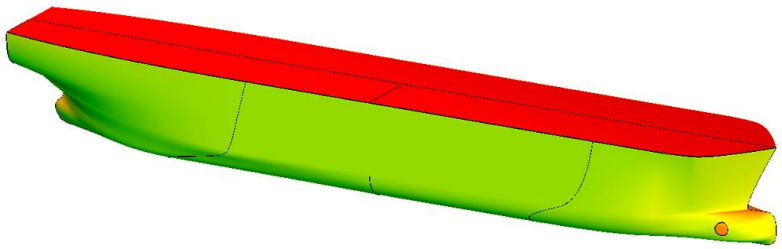

Fig. 3.5. 3D view of the ship

Determining the main projection plans, as well as a correct interpretation of the data provided by the lines plan, is an indispensable competence for the marine officer, thus offering the opportunity to optimize the time of the cargo load-unload process, as well as a better knowledge of the structure of the ship.

3.2.2. Calculation of squat for the general cargo ship

The general cargo ship (shown in subchapter 3.2.1.) was used to calculate the squat at different speeds in trapezoidal canals of different sizes. Vessel speed, V_K, was increased progessively from 0 to 15 knots (approximately 7.7 m/s). Also, for calculating the blockage factor S, the ship's breadth, draft and canal dimensions have been taken into account.

The considered theoretical canal was varied from the dimensions of a wide and deep waterway to very restrictive conditions, with a under keel clearance of only a few percent of the ship's draft. Therefore, the width at the bottom, W, was varied from $1.05 \cdot b$ to $2.50 \cdot b$ (b – ship's breadth), and the depth, h, from $1.05 \cdot T$ to $1.50 \cdot T$ (T – ship's draft) (fig. 3.6). The water surface width of the canal (W_0) was considered to be 3 times the bottom width (W); exception makes the last situation analyzed, where it was 2.5 times the bottom width.

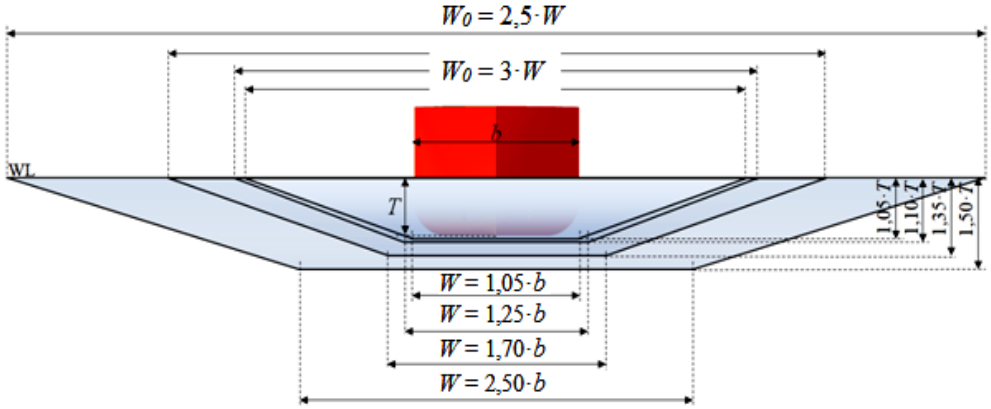

Fig. 3.6. Trapezoidal canal configurations

Analyzing the squat for all canal configurations and ship model speeds, four charts (fig. 3.7) were obtained for each considered depth. In the case of the first configuration of the canal (fig. 3.7.a) it can be noticed that at 4 knots the ship is already grounded. The under keel clearance increases to 0.65 m when the depth of the channel is $1.10 \cdot T$ (fig. 3.7.b). For each canal width, the ship's grounding occurs at 5.66 knots (for $W = 1.05 \cdot b$), 6.08 knots (for $W = 1.25 \cdot b$), 6.85 knots (for $W = 1.70 \cdot b$) and 7.55 knots (for $W = 2.50 \cdot b$).

Increasing the water depth has the effect of increasing the under keel clearance, and at larger canal widths, the risk of ship grounding is diminished for higher speeds. Thus, the under keel clearance increases to 2.275 m for the situation where the depth of the channel is $1.35 \cdot T$ (fig. 3.7.c). For the last depth considered ($1.5 \cdot T$) (fig. 3.7.d) the under keel clearance increases to 3.25 m and grounding occurs for the narrowest canal ($1.05 \cdot b$) at the speed of 13.91 knots and for the $W = 1.25 \cdot b$ width canal at the speed of 14.89 knots. For the two remaining widths, the ship can pass through the canal without grounding.

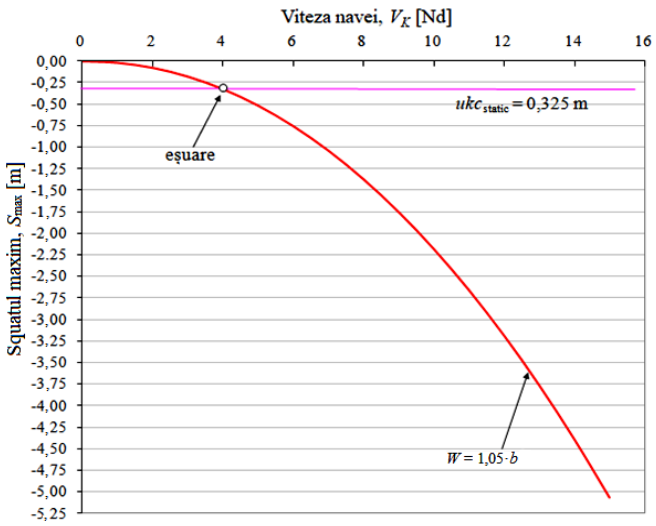

(a) $h = 1.05 \cdot T$

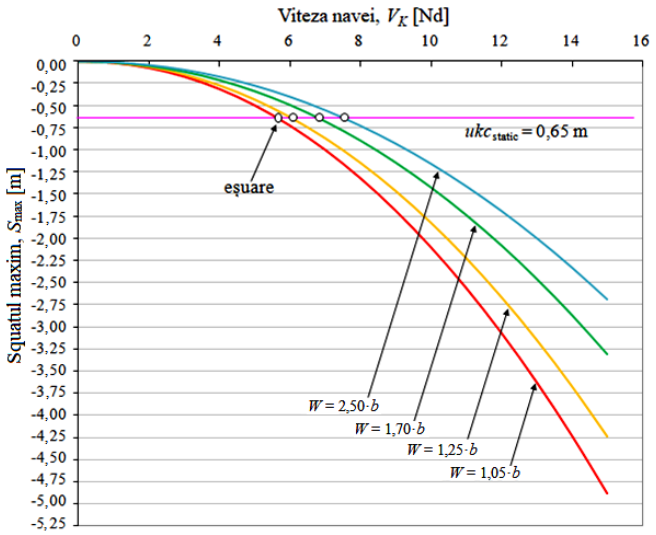

(b) $h = 1.10 \cdot T$

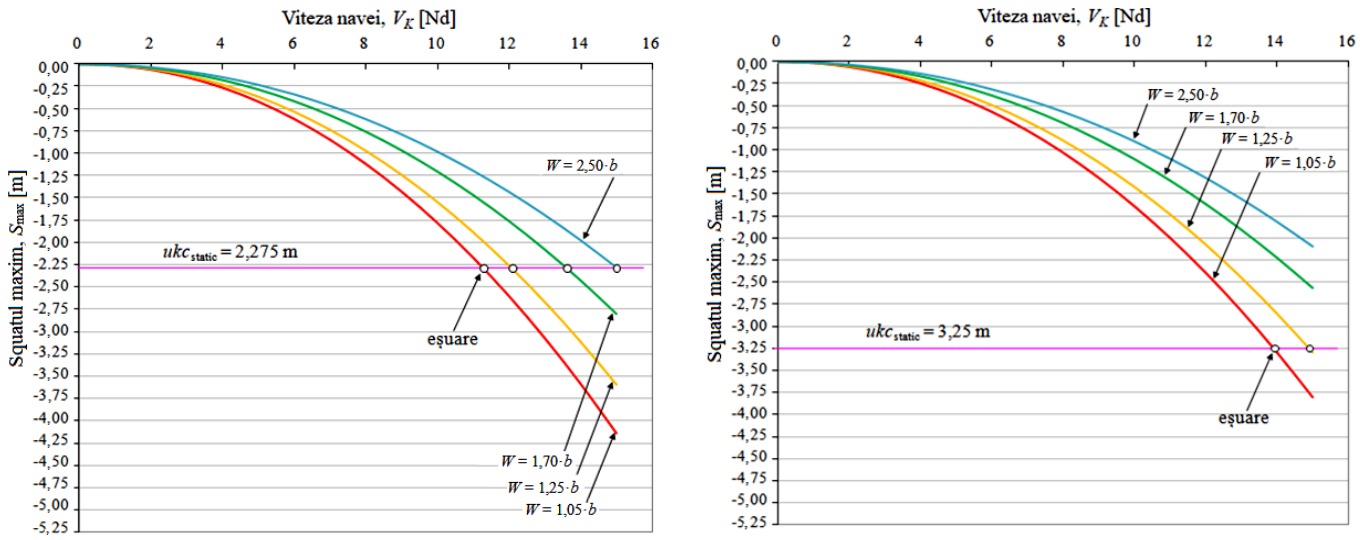

(c) $h = 1.35 \cdot T$ **(d) $h = 1.50 \cdot T$**

Fig. 3.7. Squat variation depending on ship's speed for each depth and width of the considered canal

CHAPTER 4
STUDY OF SHIP-TO-SHIP AND SHIP-TO-SHORE INTERACTION IN CANALS

4.1. SHIP INTERACTION. CAUSES AND EFFECTS

4.1.1. Ships hydrodynamic pressure domain

Ship interaction is a phenomenon associated with ship squat and has been the subject of scientific research for a long time. Generally, most studies are based on empirical formulas, experimental tools or numerical techniques (CFD), of which the first two are most commonly used.

Meeting situations in shallow waters may cause significant ship deviation from the coarse and may affect safety of navigation if they are not understood, anticipated and corrected. In navigation, the interaction occurs when the pressure fields around the vessels interact.

The interaction effects are multiple, some with serious consequences for the ship, such as grounding or collision. The cause of these effects is the interaction between the hydrodynamic pressure fields produced by the vessels during their movement. A moving vessel has two positive pressure bulbs at bow and stern and along the hull a negative pressure field, which form together an elliptical domain (fig. 4.1). When these pressure domains of the vessels come in contact there are visible effects, which become more pronounced in shallow waters.

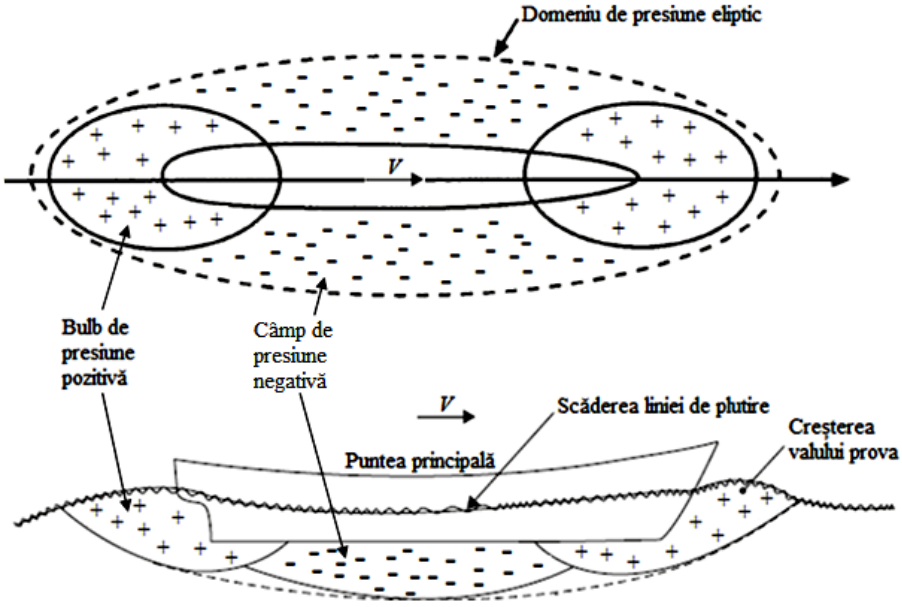

Fig. 4.1. Distribution of pressure bulbs around the hull of a moving ship (processing after *Barrass* [3])

4.1.2. Ship-to-ground interaction in canals

It has been noticed that in confined conditions, ship squat, which occurs anyway when the ship moves, increases when the vessels pass one by the other.

Moreover, when ships pass one next to each other, squat affects their trim, but also a transverse squat appears which tilts the ships into one of the sides.

4.1.3. Ship-to-ship interaction in canals

Intense maritime traffic, replenishment at sea and ship operations in ports are characterized by more and more frequent ship-to-ship interactions. Interaction between vessels is more pronounced at high speeds, a small distance between them and a low under keel clearance. It must be remembered that a correct cruising speed and a sufficiently distance between ships are indispensable to avoid or minimize the effects of interaction [3].

4.1.3.1. *Ships meeting in a canal*

From the point of view of ship interaction, the passing of ships to each other is rapid, often lacking the time to react to the forces and moments that appear. The main effect felt by ships is a moment of rotation around the vertical axis pushing the bow towards the canal bank. When ship bows interact, the moment created is weaker and easier to control, but when ships take distance, it becomes stronger and if not anticipated may cause to one of the ship a suddenly deviation into the adjacent bank (fig. 4.2) [3].

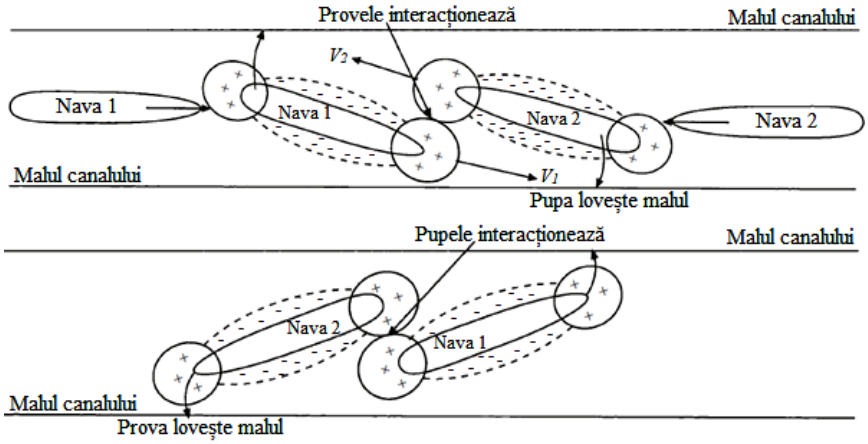

Fig. 4.2. Ship-to-ship interaction in a canal. The *approach* situation (processing after *Barrass* [3])

4.1.3.2. *Ships overtaking in a canal*

The overtaking maneuver should always be done with caution, because the relative speed is small and the ships are close enough for the interaction effects to take place. As a result of this maneuver, the collision may result, which can be avoided by a sufficient distance between the ships.

The interaction of vessels during overtaking depends on relative speed; the lower it is, the longer the effects occur. If the relative speed is zero, the vessels are moving in parallel, as is the case of refueling operations carried out by the military ships. In this situation the interaction effects must be known to find a convenient position during the maneuver [3].

4.1.3.3. *Ship-to-tug interaction in a canal*

During maneuvers in narrow channels, a tug can be found in one of the following cases:

- *Case 1*: The tugboat is at the stern of the assisted ship in the portside. The pressure fields of the ships come into contact and the interaction appears. The positive pressure bulb of the tug is rejected by the positive pressure bulb of the assisted ship. Both ships drift toward port side.
- *Case 2*: The tug is at amidships of assisted ship in port side, and is in danger of being attracted to the hull due to interaction of negative pressure bulbs. The side suction force varies with the tonnage difference between the two ships. Each ship suffers a transverse tilt.
- *Case 3*: The tug is in the bow of the assisted ship in port side. Positive pressure bulbs are rejecting, and ships deviate to starboard side. The tugboat having a higher rate of turn, there is a real danger that it is drawn in front of the ship and to be capsized.

4.1.3.4. *Ship-to-moored ship interaction in a canal*

The effects of interaction may also occur if one of the ships is moored along a quay in the overtaking maneuver. The same phenomena, forces and moments occur between the two ships, but the moored ship will move forward or back along the quay.

In general, the speed of passage to the moored vessels must be reduced, and in canals where the under keel clearance is reduced, it must be lowered to the limit that the ship can be governed. Also, the lateral distance to the mooring vessels must be large enough to allow a safe passage [3].

4.1.4. Ship-to-shore interaction in canals

When navigating in narrow waterways or canals, the flow along the ship's hull becomes very complex and interactions occur between the ship and the canal banks, due to the additional hydrodynamic forces and moments generated by the vicinity of the banks, thus affecting the movement of the ship. This phenomenon is called a *bank effect*.

In figure 4.3, it can be noted that the ship is closer to the canal bank at stern starboard side, while the port side is free. When the ship passes along the canal at a considerable speed parallel to the bank, the water passes from the bow area where the space is larger to the stern, where the area is narrower. Increased flow rate produces a drop in pressure in the Z_s zone relative to the port side area Z_p. Consequently, water pressure from port side pushes the ship's aft towards the canal's bank, causing a movement of the bow to the center of the canal. The bank effect depends on many parameters, such as bank shape, water depth, ship-to-shore distance, ship size, ship speed and propeller action. A credible estimate of the bank effect is important for determining the limit conditions a ship can operate in a canal.

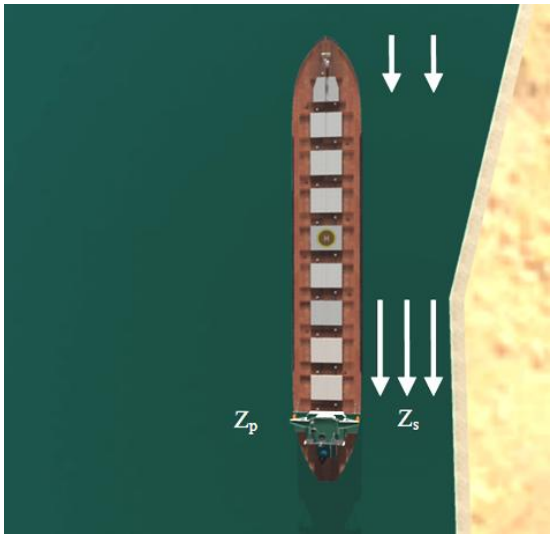

Fig. 4.3. Water flow due to bank inequality

4.2. CASE STUDY ON SHIP-TO-SHIP INTERACTION USING THE NTPRO 5000 NAVIGATION SIMULATOR

4.2.1. Initial conditions of the simulated situation

The ship-to-ship interaction simulation was performed using the NTPRO 5000 navigation and maneuvering simulator. Because ship-to-ship interaction has a greater effect in confined conditions, a 390 m width section of the Suez Canal was chosen for the simulation.

For simulation, an oil tanker and a bulk carrier were used. The characteristics of the two vessels are presented in table 4.1.

Table 4.1. Ship's characteristics

Characteristic	Oil tanker	Bulk carrier
Displacement [t]	77,100	104,510
Length [m]	242.8	250
Breadth [m]	32.2	43
Draft [m]	12.5	12.0
Maximum speed [knots]	15	14.8

This case study simulated the meeting of ships on parallel courses but of opposite directions. The lateral distance between the vessels at the time of the meeting was 50 m (fig. 4.4), and the speed was considered constant.

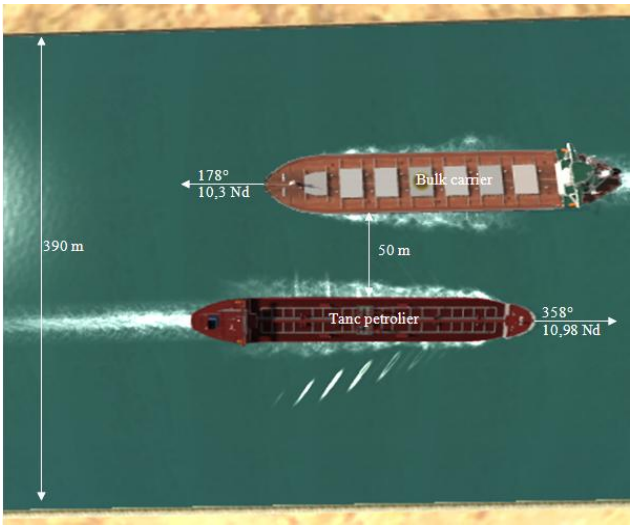

Fig. 4.4. Ships meeting on the considered canal

4.2.2. Obtained results

The subject of hydrodynamic parameters analysis, during the meeting maneuver, was the oil tanker. Under static conditions, the ship has a draft of 12.5 m both at bow and stern, but at speed of 10.98 knots (5.63 m/s) through the shallow water canal, the draft increases due to squat, reaching 13.266 m at bow and 13.308 m at stern. At the time of meeting with the bulk carrier, there is a further increase in the draft both at bow and stern.

In connection with ship-to-ship interaction and squat effect, an increase in velocity was also observed (fig. 4.5). The ship's speed has an ascending trend similar to the drafts; after a slight decrease at the time of the meeting, ship's speed increases from 10.953 knots to 11.093 knots. The oil tanker speed continues to increase as the ships move away, but this time because of the bank effect, as the ship was derived to starboard side, towards the adjacent canal bank.

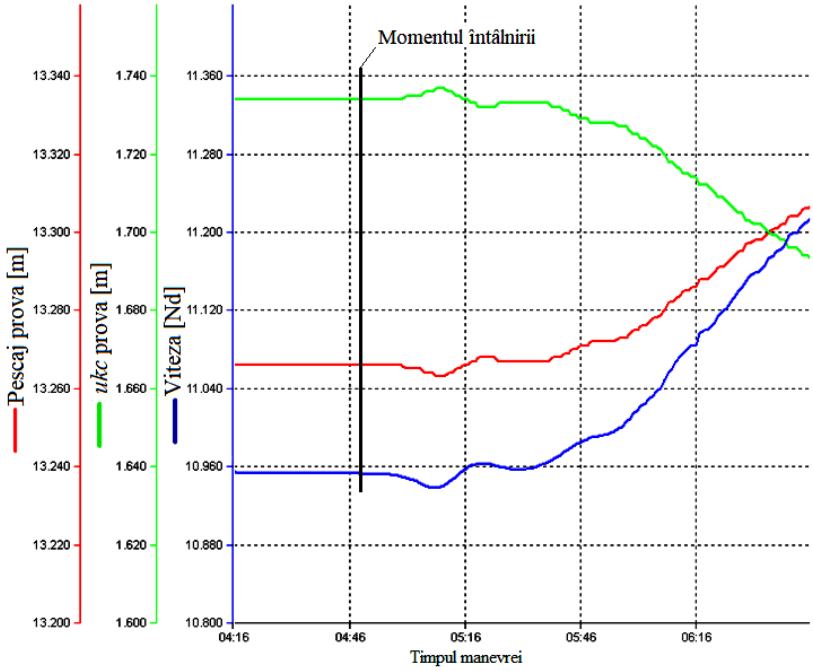

Fig. 4.5. Bow draft, under keel clearance and speed variations for the oil tanker during the meeting maneuver

When approaching, ships tend to reject each other because of the positive pressure bulbs in the bow and each one deviates towards the adjacent bank. During the maneuver, the resulting pivoting moment decreases as the positive pressure from the bow of each ship produces a lower force on the other one. When the sterns interact, the tendency of the ships is to diverge to the opposite bank, but the pivoting point is too small to produce a visible effect on the ships.

4.3. CASE STUDY ON SHIP-TO-SHORE INTERACTION IN CANALS USING THE NTPRO 5000 NAVIGATION SIMULATOR

4.3.1. Initial conditions of the simulated situations

The case study on ship-to-shore interactions using the NTPRO 5000 navigation simulator was conducted on a 476 m wide navigable waterway of the Suez Canal.

The main parameters in ship-to-shore interaction are the width – draft and length – width ratios, the distance from the centerline to the canal bank y_{ch}, the distance from one of the sides to the center of the canal e_{ch} (fig. 4.6), the angle between the ship's longitudinal plane and canal bank, ship speed V_K, but also canal width B, water depth h or canal bank slope θ.

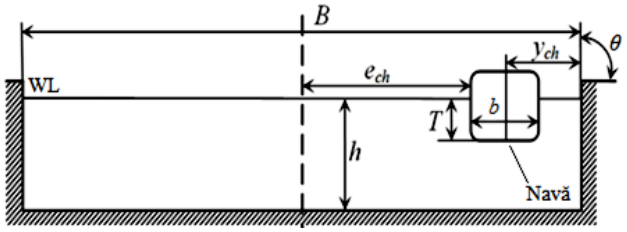

Fig. 4.6. The main geometric parameters that determine the movement of a vessel in a canal

The tests were carried out on a bulk carrier of 76,800 tones. Straight line passes were conducted through the canal on a distance of one nautical mile at different ship speeds and three under keel clearances, 10, 35 and 50% of the static draft. The distance from the ship's centerline to the canal bank, y_{ch}, was set to 58 m.

The combinations of V_K speed and h/T ratio are shown in table 4.2. The trials were performed for real-scale speeds of 6.2, 7.4, 10.3, 11.8 and 16 knots.

Table 4.2. Test condition matrix

h/T \ V_K	6.2 knots	7.4 knots	10.3 knots	11.8 knots	16.0 knots
1.10 (ukc = 10 %·T)	O	O	O	O	
1.35 (ukc = 35 %·T)		O			
1.50 (ukc = 50 %·T)		O			O

The water depth in the area was considered constant for all three under keel clearances and set so that, taking into account the ship's draft, the shallow water condition would be met in order for the ship to be affected by the squat phenomenon.

4.3.2. Results and discussions

The first trial was performed at a speed of 6.2 knots for a water depth of 1.1·T. The vessel's drafts at bow and stern are constant due to the constant depth, but their maximum value of 5.748 m at the bow and 9.462 m at the aft, respectively, is higher than the static draft. The difference between draft values represents the squat caused by the ship's speed, the reduced under keel clearance and the ship-to-shore interaction.

Regarding the hydrodynamic parameters of the ship when it moves along the bank, account was taken of the lateral and longitudinal forces acting on the hull, the pivotal moment around the vertical axis and the lateral deviation.

The ship's trajectory in this test and the final position can be seen in figure 4.7.

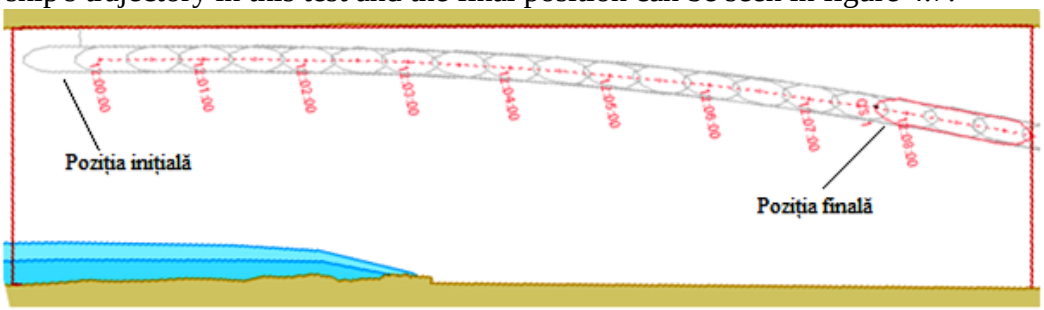

Fig. 4.7. Vessel trajectory at 6.2 knots

For the second considered speed of 7.4 knots, trials were performed for all three water under keel reserves. Studying the ship's trajectory at this speed, it was observed that there are no notable differences

between the considered depths. Figure 4.8 shows the ship's trajectory valid for all three cases, and it can be concluded that the depth of the water has a reduced effect on the final ship-to-shore distance, as compared to the effect of the ship's speed, which produces the draft increase. Compared to the first situation (fig. 4.7), the final ship-to-shore distance is higher at the end of the exercise, which means that at higher ship speeds the bank effect is more pronounced, thus pushing the ship further towards the opposite bank of the canal .

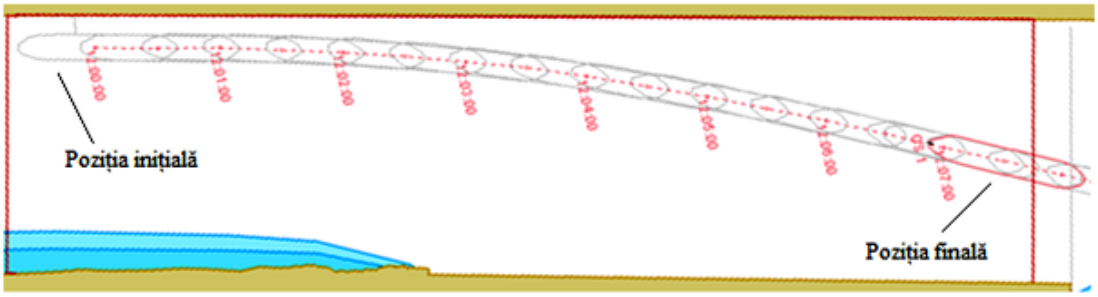

Fig. 4.8. Vessel trajectory at 7.4 knots

For the third speed (10.3 knots), the maximum drafts are 5.927 m at the bow and 9.701 m at the aft due to the low under keel clearance and the presence of the bank. As the ship's distance increases, the draft starts to drop slightly. At this speed, the ship must pay particular attention to the stern under keel clearance of only 0.5 m. At the speed of 11.8 knots, the draft is 6.046 m at the bow and 9.86 m at the aft, while the under keel clearance is 4.154 m at the bow and only 0.34 m at the stern.

For the 16 knot speed, the draft increases to a maximum of 5.987 m at the bow and 9.995 m at a stern, but because the water depth is $1.5 \cdot T$, the under keel clearances of 3,9 m at the stern and 7.97 m at the bow are safe for transit through the canal. There is a slight decrease in the draft both at bow and stern, but at the end of the simulation, when the ship approaches the opposite bank of the canal, it suffers a sudden increase.

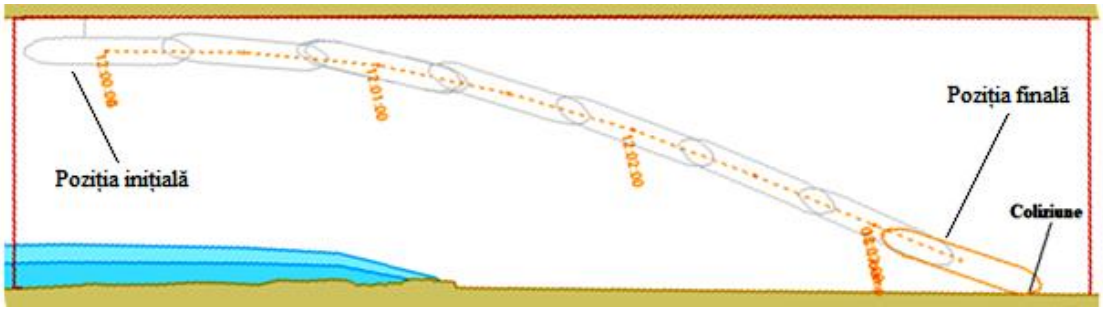

Fig. 4.9. Vessel trajectory at 16 knots

The ship's trajectory and its final position after the collision with the opposite bank can be seen in figure 4.9. It is noted that, as compared to the previously studied situations, the ship starts to distance itself from the adjacent bank much earlier because of the higher speed and the cushion effect is stronger, which makes the ship's trajectory diverted to the opposite bank where the collision occurs, this time up to the one nautical mile canal limit.

CHAPTER 5
EXPERIMENTAL RESEARCH ON BOARD TRAINING SHIP "MIRCEA"

5.1. TRAINING SHIP "MIRCEA". TECHNICAL SPECIFICATIONS

Training ship "MIRCEA" is a 44-meter height, sailing vessel, class A, with 23 sails of a total area of 1750 m^2.

The construction and technical characteristics of the ship are presented, as follows:

- **Ship's type**: the ship is a training sailing ship, with the possibility of mechanical propulsion by means of an adjustable pitch propeller driven by the engine.

- **The body** is made entirely of metal. The shape of the body is of a sailing ship, with a massive metal keel. The ship is provided with solid ballast[15].
- **Maximum length**: 81.60 m
- **Length between perpendiculars**: 62.00 m
- **Maximum amidships width**: 12.00 m
- **Construction height**: 7.300 m
- **Calculated draft at the lower edge of the keel**: 5.350 m
- **Block coefficient of fineness** (relative to L_{pp}): 0.473
- **Maximum engine speed**: 9.5 knots [35].

5.2. EXPERIMENTAL RESEARCH ON BOARD TRAINING SHIP "MIRCEA"

5.2.1. Training ship "MIRCEA" voyage – 2015

Between 01.07.2015 – 10.08.2015, sailing ship "MIRCEA" conducted an international training voyage with the students from the Naval Academy and the students of the Military School of Petty Officers of the Naval Forces "Amiral Ion Murgescu", departing from the port of Constanța and stops at the Civitavecchia (Italy), Barcelona (Spain), Marseilles (France) and Bar (Montenegro) ports.

In this voyage, the author of this thesis has served as a training instructor and an officer od the watch. On that occasion, he made a series of measurements on ship's draft, water depth below keel and ship's speed when entering and exit from those ports of call, since these areas represented more or less the characteristics of restrictive areas (shallow water and/or confined channel) that could favor the occurrence of squat.

5.2.2. Description of measurement methods

In the harbor, during the ship's in-port maneuver until the quay maneuver and during the maneuver of departure from the quay to the time of harbor departure, measurements were made on closely related parameters to the phenomenon of squat: ship's draft, water depth below keel and speed.

On board, the ship's draft shall be determined by direct reading of the draft scales at the stern (fig. 5.1) or at the ship's bow.

Fig. 5.1. Stern draft scale

As a rule, reading the drafts is done before the ship leaves the quay through direct observation from the shore. When the ship is underway, the bow draft can be read from the deck, but the stern draft cannot be read because the draft scale is not visible. To eliminate this problem, a Midland XTC 200 720p HD camcorder was used to record the stern draft variation, which was mounted on a 4 m long wood extension rod (fig. 5.2) attached to the tailgate railing.

[15] ballast – a naval term designating a series of heavy or seawater in ballast tanks loaded on a ship under certain circumstances in order to improve its navigability conditions

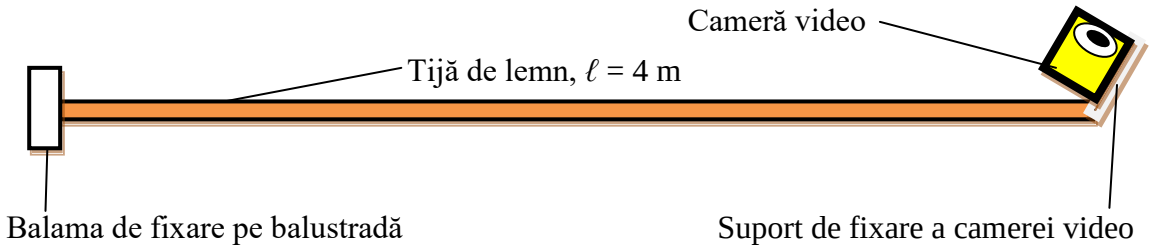

Fig. 5.2. Extension rod

At the same time, water depth below keel data of transiting area was collected from the Sperry ES 5000 echo sounder[16] with which the ship is equipped. It accurately measures depths in shallow or deep waters with 4 operating scales from 10 m to 2000 m and displays them as a depth graph on an LCD display. For continuous depth recording, the echo sounder provides the ability to print the graph on paper. Thus, the depth below keel was extracted from the graph for different moments of time, which was then correlated with the recorded draft using the camcorder.

The ship's position, coarse and speed were taken electronically from the electronic charts system, which receives this information from the GPS receiver.

5.2.3. Processing of the data obtained

As a result of the measurements in each port, the study of video footage and the extraction of depth data, by correlating them over time, information was obtained based on which analyzes were made.

For port entry maneuvers, the initial time t for data extraction shall be considered for each case, the moment when the ship has doubled the port's entry lighthouse and the end of the measurement period is considered when the ship has a 3 knots speed.

In the port exit maneuvers, the initial moment is considered when the ship exceeds the 3 knots speed and the end of the period when the ship doubles the entry lighthouse of the port. Data extraction was done at 30 second intervals.

5.3. OBTAINED RESULTS

5.3.1. Port of Civitavecchia, Italy

According to ITTC[17] [35], the shallow water condition is achieved if the ratio of the water depth h and the mean draft of the vessel T fulfills the condition of $1.2 < h/T < 1.5$. If $h/T < 1.2$, then the ship is in very shallow water.

At the entrance to the Civitavecchia harbor, the depth below keel – obtained from the ship's echo sounder, the stern draft – obtained from the video recordings and the bow draft by direct observation were measured. At the entrance maneuver, the values of h/T ratio vary between 2.68 and 4.27, so they do not fall within the limits required to meet the shallow water condition shown above, so the calculation of the ship's squat makes no sense.

The width of influence F_B for sailing ship "MIRCEA" is 215.83 m. However, the ship moves to the center of the navigable channel, both at the port entrance and at the exit, so that the width of the influence is not violated by quays or berths and thus the ship movement is not affected. At the exit of the Civitavecchia port the situation is similar because h/T ratio values vary between 2.58 and 4.27, so squat does not occur.

5.3.2. Port of Barcelona, Spain

At the entrance to Barcelona, the same measurements were made as in the previous case. The mean calculated draft was 5.325 m, as the bow draft was constantly 5.3 m, and the stern draft varied between 5.3 and 5.35 m. It is noted that, at the entering maneuver, the h/T ratio values ranges between 2.31 and 4.66, so they do not fall within the limits required to meet the shallow water condition shown above.

In this case, the width of influence F_B is 216.42 m. Although the ship moves to the center of the navigable channel, the limits of the width of the influence are sometimes broken by the dams or docks in the port, but because the average speed of the ship at the entrance is 3.74 knots, and at the exit of 4.24 knots, very low speeds, the movement of the ship is not influenced by the presence of obstacles, and the

[16] sondă ultrason – aparat de navigatie maritimă destinat măsurării adâncimii apei (sub chila navei), folosind ultrasunete
[17] International Towing Tank Conference

squat does not occur. At the exit from Barcelona, the situation is similar because *h/T* ratio values vary between 1.995 and 3.12.

5.3.3. Port of Marseille, France

The same measurements were made at Marseilles port as in the previous cases. At the entrance maneuver, the mean calculated draft was 5.3 m, because the bow and stern were constantly 5.3 m. At the exit of the port, the mean draft was 5.35 m because the bow draft was constantly 5.3 m and the stern draft varied between 5.35 and 5.5 m. Thus, at each time interval, the water depth *h* and the *h/T* ratio were calculated. It can be seen that, when entering, the values of this ratio vary between 2.339 and 2.905, so they do not fall within the limits required to meet the shallow water condition shown above.

In this case, the width of influence F_B is 217 m. The width of influence limit from the starboard side is violated, on a small portion, by the entrance dike, but because the average ship's speed when entering is 3.82 knots, and 4.67 knots at departure, very low speeds, the ship's movement is not influenced by the presence of this obstacle, and the squat does not occur. On port of Marseille departure, the situation is similar because *h/T* ratio values vary between 2.23 and 4.31.

5.3.4. Port of Bar, Montenegro

At the entrance to the Bar harbor, the same measurements were made as in the previous cases. The mean draft was 5.325 m as the bow draft was constantly 5.3 m, and the stern draft ranged between 5.3 and 5.35 m. When entering, *h/T* ratio values ranges between 2.99 and 3.62, so they do not fall within the limits required to meet the shallow water condition previously described.

In this case, the width of influence F_B is 216.41 m. The width of the influence port side limit is violated, on a small portion, by a dike, but due to the fact that the ship's average speed is 3.44 knots at arrival, and 4.04 knots at departure, very low speeds, the ship's movement is not influenced by the presence of this obstacle, and the squat does not occur. At Bar harbor exit, the situation is similar because *h/T* ratio values vary between 2.427 and 3.14, so squat does not occur.

The ship's route on the electronic chart during data recording is shown in figures 5.3.a, b for the entering maneuver. The total distance traveled between the two moments is 531 m, while the ship's speed reached a maximum of 3.8 knots.

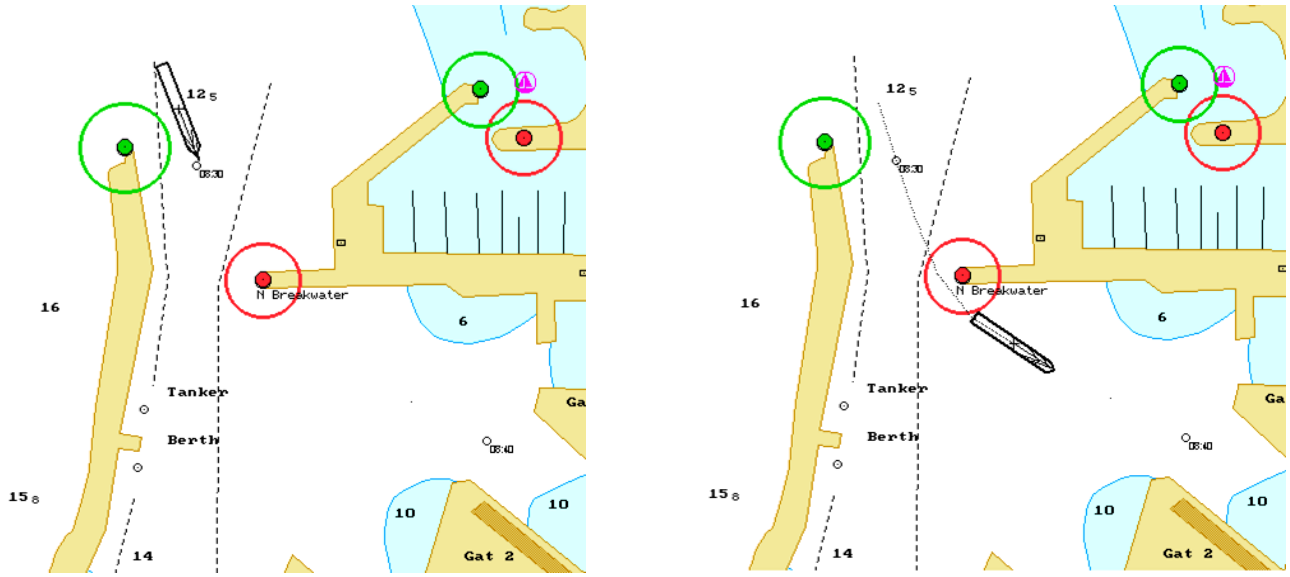

(a) Ship's position at the beginning of the maneuver (b) Ship's position at the end of the maneuver

Fig. 5.3. Entrance maneuver at Bar harbor

5.4. CONCLUSIONS

Following measurements and interpretation of the results, the following conclusions were drawn:

- the only way on board the vessel to measure the draft is through direct observation of the draft scales. Therefore, for reading the stern draft, which is harder to read, a video camera and an extension rod were used to record the variation of the draft and its subsequent viewing.
- in terms of the measurement methods used, it was identified a difficulty in timing synchronization of drafts with the depth diagram obtained from the echo sounder and the ship's speed from the electronic charts system was identified on board and then, on the interpretation of the data obtained, due to the fact that this information comes from different navigation equipment with offset internal clocks.

- the attempts to capture a noticeable change of draft due to squat proved to be unsuccessful due to several aspects:
  - first of all, the geometric parameters of sailing ship "MIRCEA", such as length, breadth, draft, but especially the block coefficient of fineness, are not suitable for carrying out these kind of experiments because their values are too small for the squat to produce, taking into consideration the ship's speeds when entering/leaving the ports.
  - secondly, for a ship of these dimensions, the squat would occur and would be visible on the draft scale if the travel speed exceeds 10 knots, but sailing ship "MIRCEA" can develop a maximum speed of 9.5 knots, and in ports the maximum speed was 6.9 knots. Under these conditions squat was not observed on any records made.
  - the characteristics of the ports were not sufficiently restrictive for this ship so as to lead to squat occurrence.
- the water depth in transit ports, as well as the navigable channel width were variable and the occurrence of squat phenomenon was hard to observe.
- another determining factor on the squat phenomenon was the variable speed of the ship. The time when the speed was constant speed was not long enough for the squat to occur and be visible.

CHAPTER 6
NUMERICAL SIMULATION OF SHALLOW WATER EFFECTS ON TRAINING SHIP "MIRCEA" HULL

6.1. INTRODUCTION

The study presented in this paper follows the process and selection of appropriate methods for geometric modeling, mathematical modeling and preliminary creation of CFD simulation with ANSYS CFX, which uses a 3D solver based on the Finite Volume Method.

Having the "MIRCEA" sailing ship lines plan, the ship's hull was geometrically shaped up to the 7 m waterline, after which the domain of fluid was defined to study depth effects on the body. These effects mainly relate to variations in pressure, speeds, forces and moments on the hull.

6.2. HULL GEOMETRY

The first step of CFD simulations is to prepare the CAD geometry of hull, which is described below. The structure of the geometry is based on the data in table 6.1. The 3D final form of the "MIRCEA" sailing ship hull used for analysis is shown in figure 6.3.

Table 6.1. Hull geometry characteristics

Parameter	U.M.	Dimension
Waterline length	L_{wl} [m]	62.061
Waterline maximum breadth	B_{wl} [m]	12.00
Construction height	D [m]	7.00
Draft	T [m]	5.35
Displacement	Δ [t]	1984.2
Block coefficient of fineness	C_B	0.486

The environment in which the ship is moving is known as the domain. A broad range has been created to avoid that the boundaries of the domain affect the flow along the hull. The dimensions of the domain (length, width, depth) around the ship are shown in figure 6.1 and are expressed in terms of hull length, L_{wl}. These dimensions are in accordance with the minimum recommendations of the International Towing Tank Conference (ITTC).

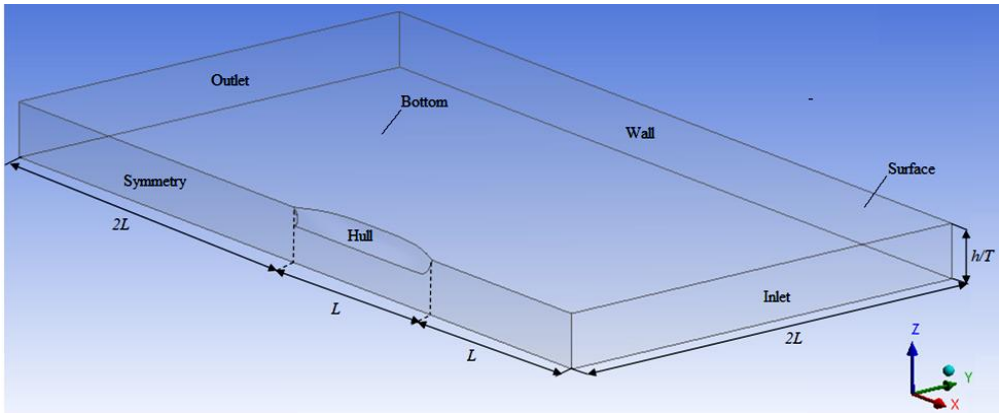

Fig. 6.1. Fluid domain dimensions

The simulations were performed on different domains of variable depth and at speeds between 2 and 8 knots (fig. 6.2). All depth and speed configurations of the performed simulations are shown in table 6.2. The 22 simulated cases start from extremely shallow water conditions (h/T = 1.1) and up to a reasonable depth but still considered shallow (h/T = 3.0).

Table 6.2. Simulations matrix

h/T \ V_K	2 knots	4 knots	6 knots	8 knots
h/T = 1.1	O	O	O	
h/T = 1.2	O	O	O	
h/T = 1.5	O	O	O	O
h/T = 2.0	O	O	O	O
h/T = 2.5	O	O	O	O
h/T = 3.0	O	O	O	O

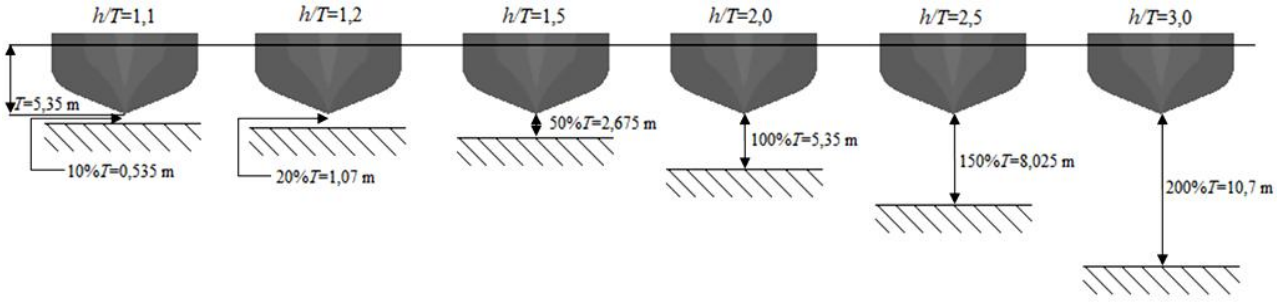

Fig. 6.2. Simulated depths configurations

Construction stages of the hull's geometry were as follows:

1. Creating 3D curves defined using points in the coordinate file;
2. Generating a surface joining these curves with the Skin/Loft function;
3. Mirroring the surface created by the *XZ* plane to generate the starboard side using the Mirror function;
4. Generating a flat surface at the 7 m draft to close the body;
5. Create a new coordinate system translated on the Z axis to – 5.35 m, to translate the body to this elevation so as to obtain the immersed body at the considered draft (fig. 6.3);
6. Enroll the body using the Enclosure function in a rectangular parallelepided that extends a ship's length from the bow, two lengths to the aft, two lengths in each board, and down from the baseline with a value corresponding to each considered depth. This parallelepiped is the fluid domain;
7. Extract the ship's body from this domain using the Boolean-Subtract function;
8. Cutting the ship's body to the new plane and erasing the emerged part, from the 5.35 m waterline to the 7 m waterline;
9. Cutting the fluid domain along the *OXZ* plane, using the Symmetry function;
10. Create domain sides using the Named Selection function as: Inlet, Outlet, Surface, Bottom, Wall, Hull and Symmetry (fig. 6.1).

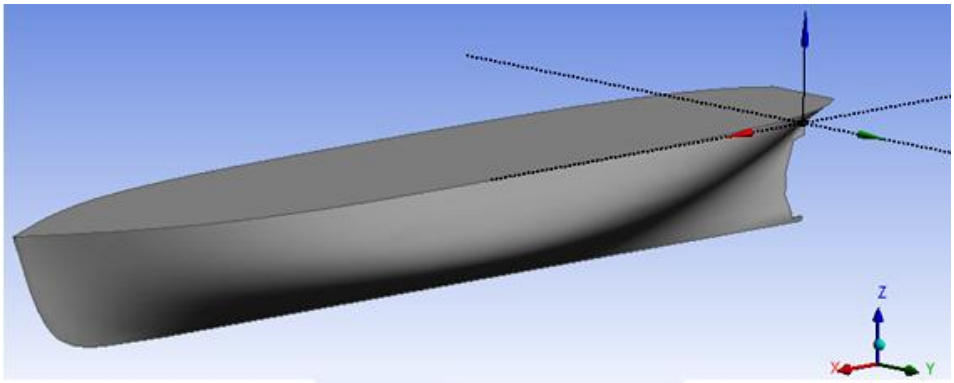

Fig. 6.3. Downward hull's translation

6.3. MESH GENERATION

The division of the computational domain into a number of cells is called a mesh. Particular attention must be paid to meshing, because a poor quality has a negative effect on the solution's convergence and confidence in the calculated results. Figure 6.4 shows the cells grid of the fluid domain in one of the studied cases.

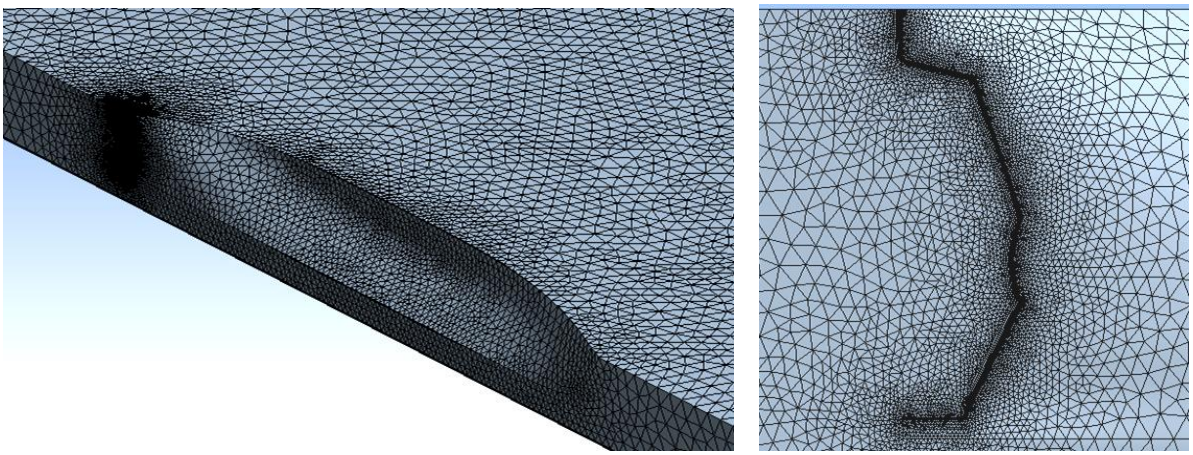

(*a*) General view (*b*) Stern zone

Fig. 6.4. Cells grid

In order to observe the flow phenomenon in simulations, the density of the mesh was more concentrated in certain regions of the domain. In this respect, a fine mesh on the surface of the hull was used and cell layers were created along it to solve the flow in the boundary layer. The additional cell layers were constructed so that the total thickness corresponded to the estimated thickness of the boundary layer and the width of the first cell layer was set to obtain an appropriate value for the y^+ parameter (presented in subchapter 6.4.5).

6.3.1. Study on mesh sensitivity

In order to determine the accuracy of the CFD solution and to maintain a low computational effort, a mesh sensitivity study was conducted. The case h/T = 2.5 was chosen with V_K = 8 knots, turbulence model *k-ω SST*[18]. The study was conducted by generating three different meshes, one coarse, one medium and one fine to determine how the grid quality affects the simulation results. The number of nodes, duration of simulations and total forces acting on the hull in *X* and *Z* directions for the chosen case are presented in table 6.3. In all three meshes, the value of the y^+ parameter is maintained at 60 on the surface of the hull, the difference between them being only the number of nodes.

Table 6.3. Mesh characteristics for h/T = 2.5, V_K = 8 knots

Mesh resolution	**Coarse mesh (M1)**	**Medium mesh (M2)**	**Fine mesh (M3)**
Nodes number	866,835	1,078,354	1,458,185
CFD simulation duration	08h 17min	14h 53min	23h 51min
Total *X* force on hull	– 1.0408e+04	– 1.0339e+04	– 1.0120e+04
Total *Z* force on hull	– 2.8221e+05	– 2.8216e+05	– 2.8176e+05

[18] shear stress transport

The value of the total force acting on the ship's hull in the *X* direction becomes smaller as the mesh becomes more refined, resulting in a value of 10,120 N for the M3 grid. The difference between the values obtained with the M1 and M2 meshes is about 2 %, but the total time of CFD simulations differs significantly from one grid to another. At the same time, the value of the total force acting on the ship's hull in the *Z* direction has a maximum value of – 281,760 N, obtained with the M3 mesh, but the difference between the other values obtained is less than 1 %. Due to the small differences and taking into account the computing time, it was concluded that the M2 medium mesh is the most appropriate and provides good results with a reasonable computational cost.

6.4. MATHEMATICAL MODEL

6.4.1. Governing equations of the mathematical model

On the equations of fluid movement derivation, the exchange rate of the fluid properties φ per mass unit and per unit volume should be known. This field is fully described by density ρ, velocity U, pressure p and viscosity v. The fluid field $\varphi(x, y, z, t)$ will be investigated using the Euler method, assuming that the properties that are relevant are in relation to the fluid particle position and time. At a given time t, the fluid particle is at the coordinate point (x, y, z) and after a time $t + \Delta t$ it moves to another coordinate point $(x + \Delta x, y + \Delta y, z + \Delta z)$.

6.4.2. Navier-Stokes equations for moment conservation

Viscous shear stresses from the moment equations may be related to the linear deformation rates of the fluid element, these being expressed by the velocity components. For an isotropic Newtonian fluid, the relationship between shear stresses and deformations rate is given by the shear stress tensor [18]

$$\overrightarrow{\Im} = \begin{pmatrix} \tau_{xx} & \tau_{yx} & \tau_{zx} \\ \tau_{xy} & \tau_{yy} & \tau_{zy} \\ \tau_{xz} & \tau_{yz} & \tau_{zz} \end{pmatrix}. \tag{6.1}$$

6.4.3. Concept of turbulence modeling

The movement of a viscous fluid is governed by the Navier-Stokes equations, which are valid for both turbulent and laminar flow. Numerical modeling of turbulence is a very difficult task, involving a profound understanding of turbulent flow physics and extensive knowledge of mathematical methods.

In this paper, the viscous flow along the hull of sailing ship "MIRCEA" is supposed to be incompressible, and the numerical problem is described by the RANS[19] equations.

6.4.4. *k-ω* turbulence model

The *k-ω* model has the advantage that it is valid in areas close to walls, as well as regions with low turbulence, which means that the transport equations can be used across the entire flow domain. A disadvantage of this model is that the results are sensitive to the choice of boundary conditions and initial conditions.

To use together the advantages of the *k-ε* and *k-ω* models, *Menter* (1994) developed the shear stress transport model (SST), combining the two models into one using mixing functions. In this hybrid model, the *k-ω* model is used in the boundary layer flow, while the *k-ε* model is used in the free flow. The model is recognized for good performance and is the most commonly used turbulence model for naval hydrodynamic simulations [25].

6.4.5. Boundary layer

To characterize the flow near the wall, a dimensionless dimension is often introduced to measure the distance to the wall. This is defined by the relationship

$$y^+ = \frac{u_* \cdot y}{\nu}, \tag{6.2} [23]$$

where y is the distance to the wall and u_* – the friction speed. The friction speed is

$$u_* = \sqrt{\frac{\tau_w}{\rho}}, \tag{6.3} [23]$$

where τ_w is wall shear stress,

[19] Reynolds averaged Navier-Stokes

$$\tau_w = \rho\nu \left.\frac{\partial U}{\partial y}\right|_{y=0} . \quad (6.4)\ [23]$$

In the boundary layer, gradients of the flow variables in the normal direction on the wall are generally very large compared to those in the free flow. This implies that a higher spatial resolution is needed by the solution of the method to surpass the effects near the wall. A common alternative method used to hinder the demands of a large spatial resolution is the use of wall functions, which are empirical models used to estimate flow variables near walls.

6.4.6. Convergence criteria

To decide if a solution has reached the desired level of convergence, it is useful to monitor the residual flow variables for each iteration. During the CFD simulations there have been used RMS[20] residuals type with a target value of 10^{-5}, which represent a good convergence and is sufficient for most engineering applications [34].

6.5. BOUNDARY CONDITIONS

Simulations were performed for 6 water depth values and 4 ship speed values, and the modeling included the following assumptions and simplifications:

- homogeneous flow of incompressible fluid;
- linear motion with constant speed;
- free surface without waves and currents;
- the width of the domain equal to four ship lengths to eliminate the wall effect;
- the ship is considered on even keel without the influence of the rudder or the propeller;
- the surface of the hull is perfectly fine;
- straight bottom without natural disturbances;
- due to flow symmetry, calculations were performed for half of the domain;
- geometric modeling of the ship was made on a natural scale;
- fluid flow was carried out in a rectangular domain around the hull of the ship (fig. 6.5).

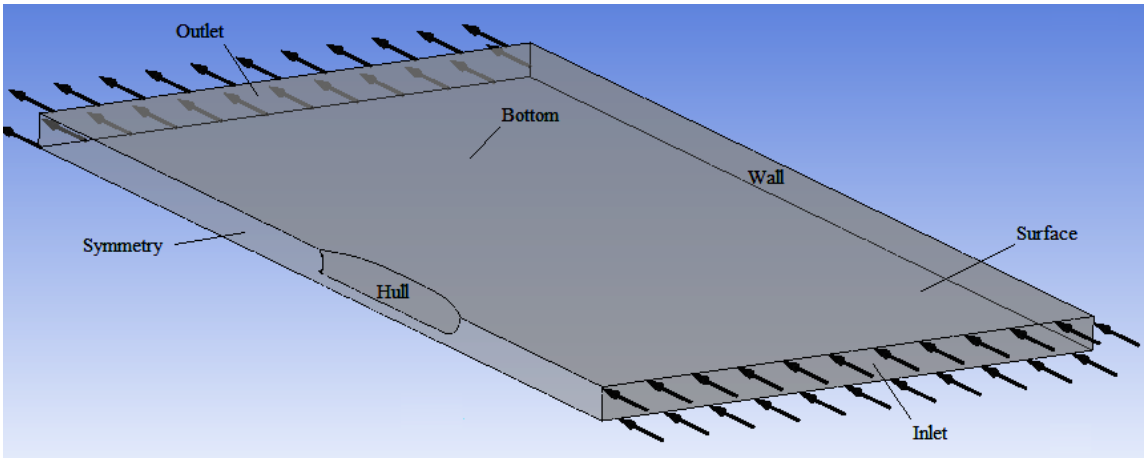

Fig. 6.5. Fluid domain limits

The limits of the computational domain are illustrated in figure 6.5 and the boundary conditions are defined as follows.

The condition imposed at the front side of the domain was *inlet* type, and the fluid velocity corresponded to the hull velocity for each simulation. The speeds for which simulations were made were 2 knots (1.029 m/s), 4 knots (2.058 m/s), 6 knots (3.087 m/s) and 8 knots (4.116 m/s). The turbulent flow variables were defined by specifying the value for turbulent intensity and the turbulent viscosity ratio. The condition imposed at the back of the domain was *outlet* type, with the *Average Static Pressure* option and the 0 Pa relative pressure. The condition imposed on the bottom was *no slip wall*. It has been assumed that the bottom of the domain moves with the speed of the ship, but in opposite direction, and for this, the *Wall Velocity* option was introduced. On the hull, it was defined the condition of *no slip wall*, *stationary* and at the surface of the field and on sides, the *free slip wall* condition. The symmetry plan was set to *symmetry* boundary condition.

[20] root mean square

6.6. SIMULATION SOLUTIONS AND RESULTS

6.6.1. Model solving

The calculations were performed with the ANSYS CFX solver. The turbulent flow was simulated by solving Reynolds-averaged Navier-Stokes equations (RANS) for incompressible flow.

The total time allocated to simulations has been calculated so that a fluid particle passes at least once the entire length of the fluid domain. The time step for each computation was 0.1 s. The calculations were performed with a single iteration each time step.

6.6.2. Numerical results

In this section, the analysis of the obtained results is done for the h/T = 1.5 case at all considered speeds, 2, 4, 6 and 8 knots, respectively, to give a picture of the speed influence in shallow waters Subsequently, cases are analyzed with the depths considered.

In table 6.4 are presented the total forces, comprised of pressure forces and viscous forces acting on the hull on the three axis at all four considered speeds. The resulting force in the X direction represents the ship's resistance, in the direction Y is the drift and in the Z direction is the vertical hydrodynamic force that causes the ship to sink due to the interaction with the bottom of the domain.

Table 6.4. Total forces acting on hull for h/T = 1.5

Speed, V_K	Axis	Type		
		Pressure Force	Viscous Force	**Total Force**
2 knots	X	– 1.8896e+06	– 6.7361e+06	– 8.6256e+03
	Y	2.1895e+04	1.4989e+01	2.1910e+04
	Z	– 2.6659e+04	– 5.4302e+00	– 26664e+04
4 knots	X	– 3.1287e+03	– 4.7776e+03	– 7.9063e+03
	Y	8.8131e+04	4.4426e+01	8.8176e+04
	Z	– 1.0688e+05	– 2.8185e+01	– 1.0691e+05
6 knots	X	– 1.5714e+03	– 5.0237e+03	– 6.5951e+03
	Y	1.9800e+05	8.8746e+01	1.9809e+05
	Z	– 2.4043e+05	– 3.7657e+01	– 24046e+05
8 knots	X	– 2.5288e+03	– 4.1342e+02	– 2.9422e+03
	Y	3.5263e+05	2.7119e+00	3.5264e+05
	Z	– 4.3170e+05	4.4192e+00	– 4.3170e+05

By comparing the contours of these forces with speed, slight differences can be observed between cases, which once again emphasize that hydrodynamic forces acting on the hull change when the vessel speeds up in shallow water conditions. The representation of forces in the Z direction, in the form of contours on the hull, can be seen in figure 6.6.

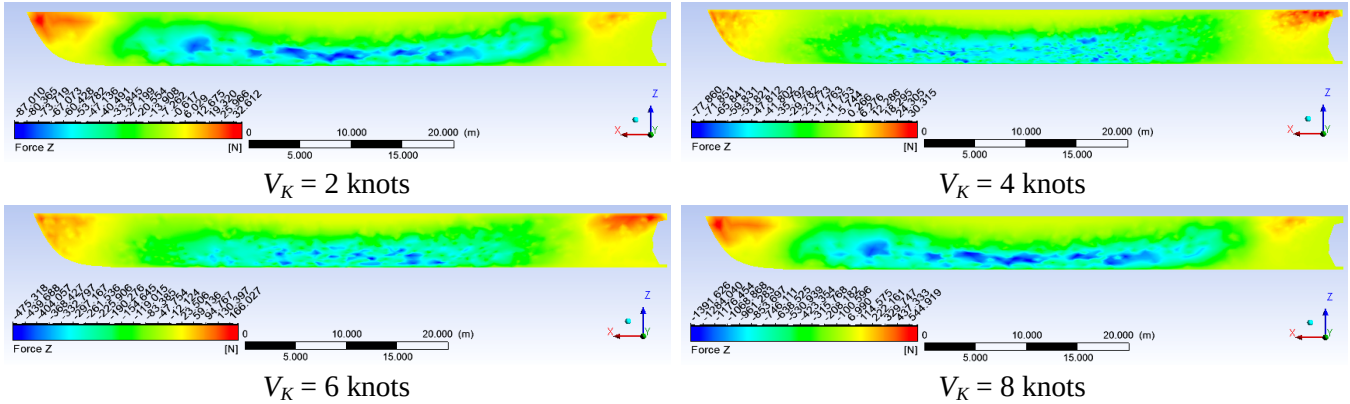

V_K = 2 knots V_K = 4 knots

V_K = 6 knots V_K = 8 knots

Fig. 6.6. Vertical forces contours (Z force)

The pressure variation on the ship's body is shown in figure 6.7, where it can be seen that its distribution is normal for a ship's body, with a positive pressure bulb in the bow and aft of the vessel and a negative pressure field on the bottom of the hull, along the body, which is consistent with the theory presented in Chapter 4.

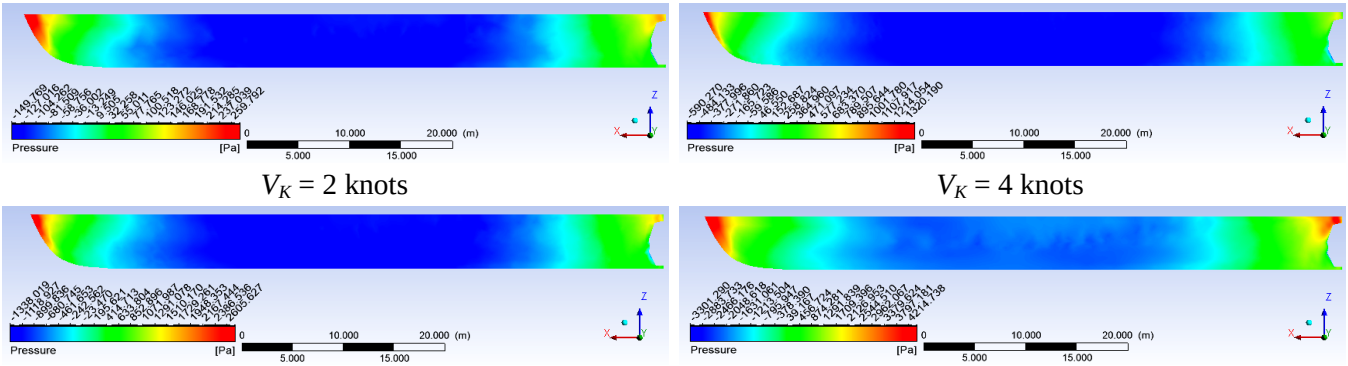

V_K = 2 knots V_K = 4 knots

V_K = 6 knots V_K = 8 knots

Fig. 6.7. Pressure contours on hull at considered speeds, h/T = 1.5

CFD post-processing enables the view of pressure variation along the keel, shown in figure 6.8. It can be observed that at all studied speeds, the maximum pressure is in the bow and the minimum is amidships. By comparing the four situations, one can conclude that a higher ship's speed causes a greater pressure drop, even if the depth is constant.

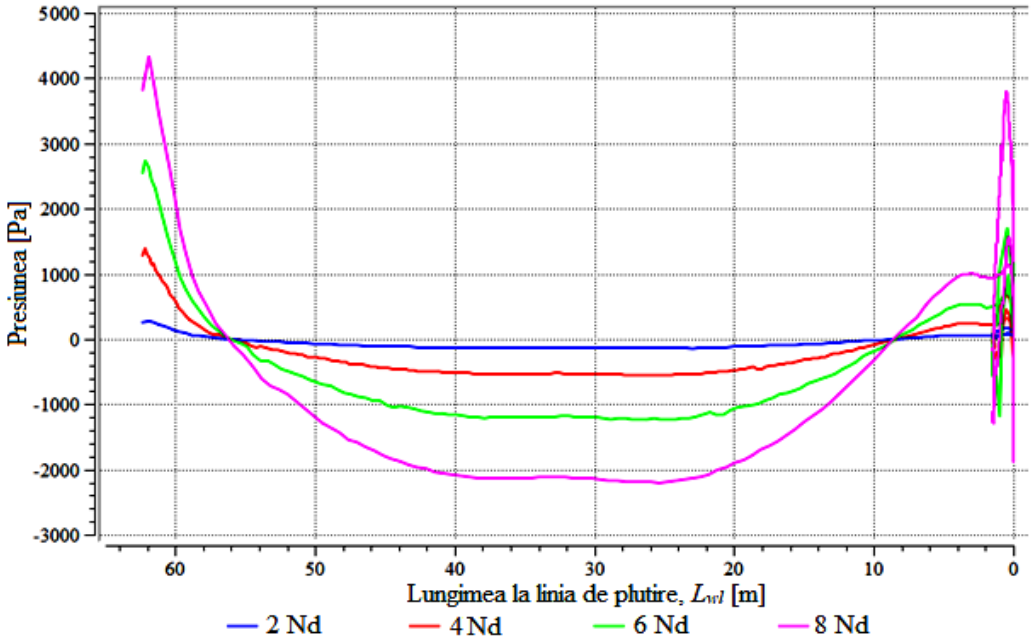

Fig. 6.8. Pressure variation along keel for h/T = 1.5

The velocity variation in the fluid domain along the hull during the simulation is shown in form of contours in figure 6.9. As expected, the potential increase in flow velocity can be observed due to the interaction between the ship's body and the field bottom. In all four cases presented, in the area between the hull and the bottom, the maximum velocity of the fluid is 12.6 % higher than the fluid velocity at the beginning of the simulation.

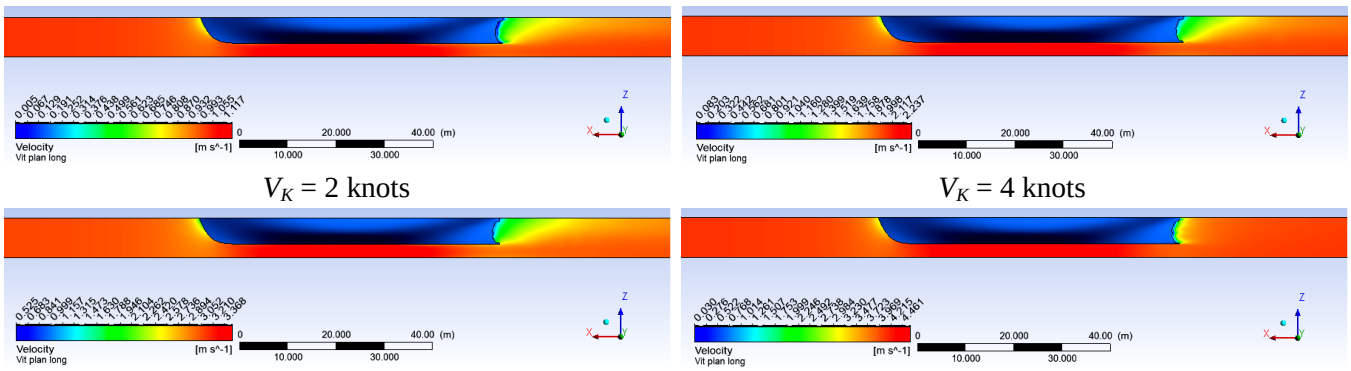

V_K = 2 knots V_K = 4 knots

V_K = 6 knots V_K = 8 knots

Fig. 6.9. Speed contours in longitudinal plane for h/T = 1.5

6.6.3. Verification and validation

To see if the method used is good and the solution is convergent, it was checked if the total mass of fluid at inlet is equal to the mass at outlet. The numerical convergence adopted for these calculations was the criterion of reducing the maximum difference between consecutive iterations of the three components of velocity and pressure below 10^{-5}.

As far as concerning the validation, there are currently no experimental data conducted on board sailing ship "MIRCEA" for validation of the simulation results, but in the literature the method used for these simulations is confirmed by simulations performed on standard ship models, such as KCS[21] or KVLCC2 Moeri tanker, which are already validated with experimental data.

6.7. SQUAT CALCULATION USING CFD METHOD AND ITS COMPARISON WITH EMPIRICAL FORMULAE

Vertical hydrodynamic forces, calculated with ANSYS CFX, were used for squat calculations; these being interpreted as total forces acting on the hull. They represent the sum of the static and dynamic buoyancy force, the latter varying according to the hydrodynamic pressure generated by the hull motion over the bottom of the domain.

It can be argued that when increasing the ship's speed in shallow waters, even extreme in some cases (h/T = 1.1 and h/T = 1.2), the vertical hydrodynamic force decreases, having larger negative values, indicating a strong interaction between the hull and the domain bottom.

Regarding the variation of the total buoyancy force in relation to depth, at the same speed, an increase is observed as the depth increases. For all speeds, the minimum force is encountered at h/T = 1.1 and the maximum at h/T = 3.0, except at 8 knots, where the minimum value is obtained at h/T = 1.5.

It can be concluded that when increasing the depth and implicitly the under keel clearance, this negative force increases, the interaction between the ship and the domain bottom is smaller and the squat effect decreases in intensity. An overview of the variation of this hydrodynamic force based on speed and depth is shown in figure 6.10.

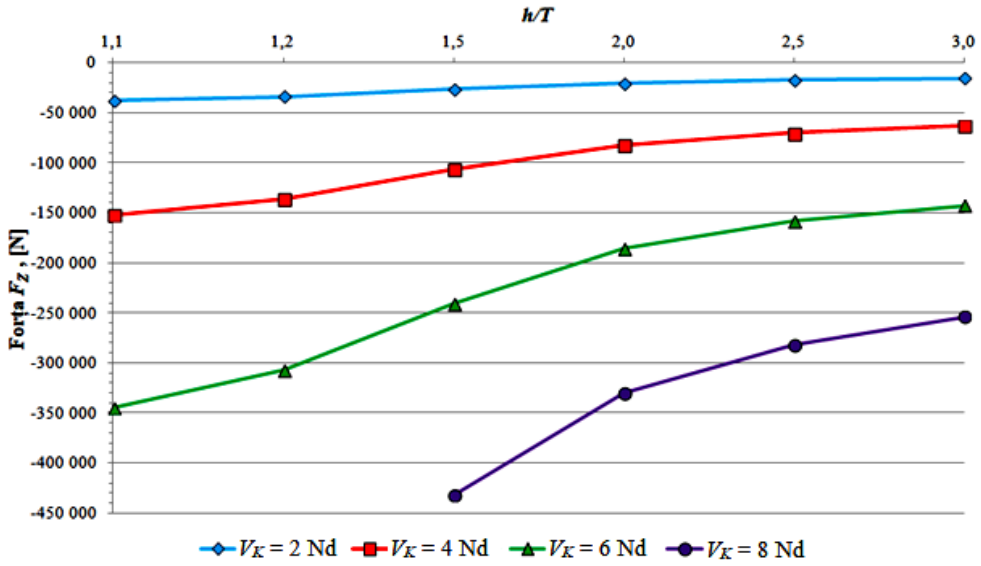

Fig. 6.10. Vertical hydrodynamic force variation vs. speed and depth

The squat was calculated for each of the 22 cases using the total buoyancy force (F_Z) values obtained in the simulations. Thus, for the hull of sailing ship "MIRCEA", the squat values presented in table 6.5 were obtained.

Table 6.5. Squat values in testing conditions

V_K \ h/T	h/T = 1.1	h/T = 1.2	h/T = 1.5	h/T = 2.0	h/T = 2.5	h/T = 3.0
2 knots	– 0.006858	– 0.006160	– 0.004821	– 0.003724	– 0.003176	– 0.002862
4 knots	– 0.027480	– 0.024670	– 0.019329	– 0.014917	– 0.012720	– 0.011462
6 knots	– 0.062316	– 0.055540	– 0.043475	– 0.033578	– 0.028635	– 0.025807
8 knots	-	-	– 0.078051	– 0.059711	– 0.050980	– 0.045932

[21] KRISO (Korea Research Institute of Ships and Ocean Engineering) Container Ship

Graphically, the variation of squat according to speed is shown in figure 6.11, for each of the six simulated depths.

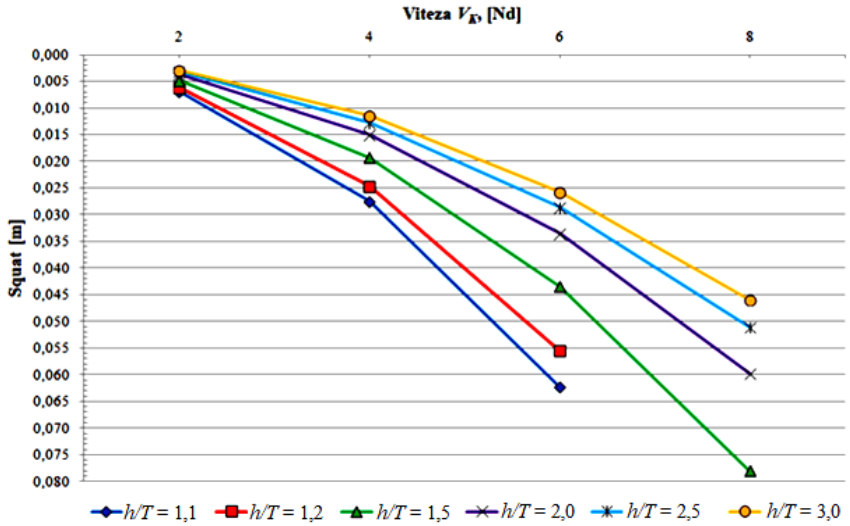

Fig. 6.11. Squat variation vs. speed and depth

In conclusion, it is noted that the variation of squat is dependent on depth and speed. Thus, the smaller the under keel clearance and the higher the speed, the more pronounced the squat is and the increase of the ship's draft. It should be emphasized, however, that the values obtained from the CFD simulations are in the order of the centimeters, values that are in accordance with ship's dimensions and considered speeds, but which may be difficult to see in reality, fact that was concluded in the experimental research carried out on board sailing ship "MIRCEA", presented in Chapter 5.

In order to evaluate the predictability of ship squat prediction using the vertical hydrodynamic forces determined with ANSYS CFX, a comparison was made with nine of the most common empirical methods for calculating squat in shallow open waters. The 9 methods are: *Barrass*, *Eryuzlu* and *Hausser*, *Eryuzlu*, *Hooft*, *Huuska*, *ICORELS*, *Yoshimura*, *Millward*, *Soukhomel* and *Zass*, which were presented in Chapter 2 of the thesis.

Figure 6.12 illustrates, for each of the considered depths, the variation of squat for all 10 methods used. Generally, there is a tendency of squat increase which is proportional to speed in all situations and for each method. As for differences between methods, it is estimated that *Barrass*'s method gives the values closest to the CFD method in all analyzed situations, and the rest of the methods overestimate squat in different proportions from one depth to another; the method of *Soukhomel* and *Zass* gives the highest squat values.

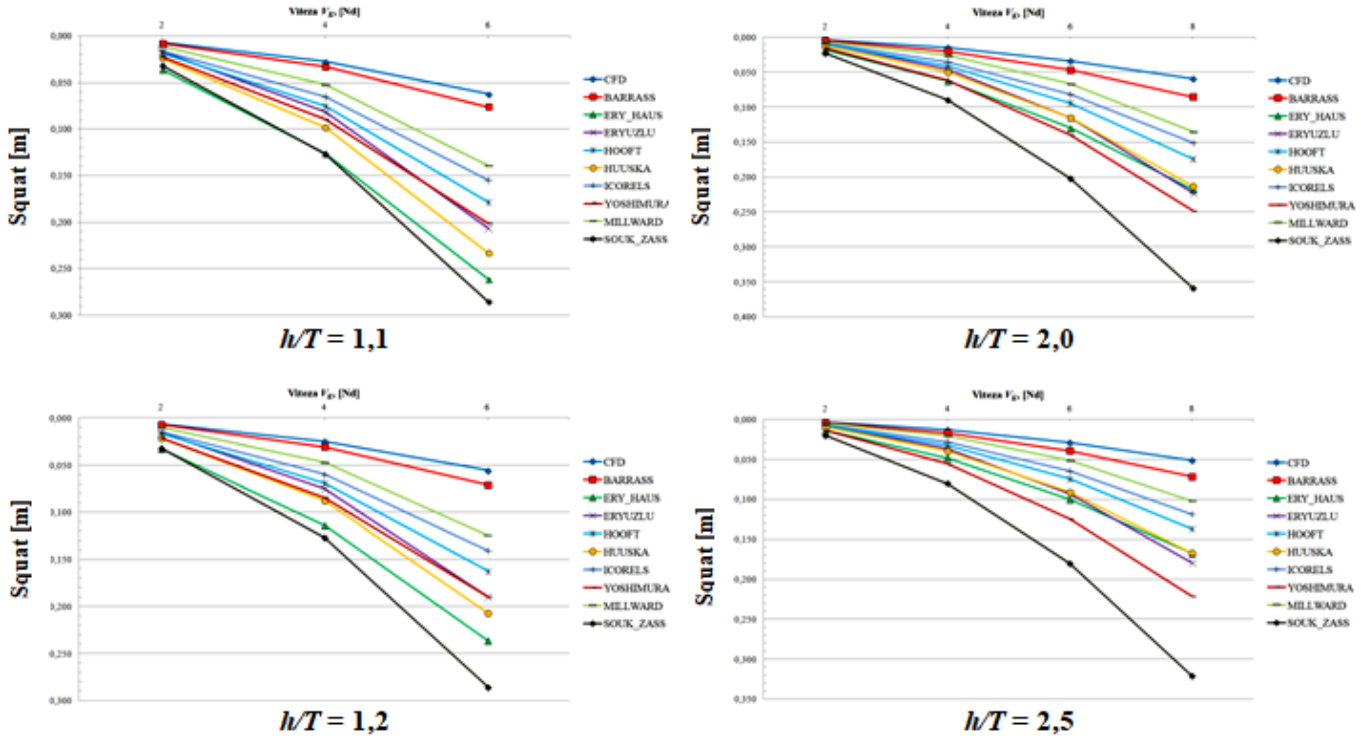

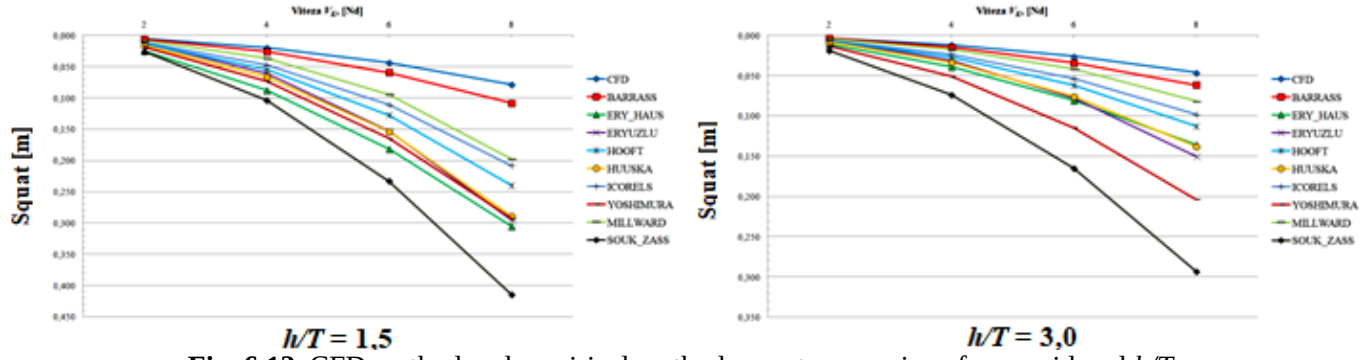

Fig. 6.12. CFD method and empirical methods squat comparison for considered *h/T*

Generally, it is appreciated that the methods that best approach the values obtained by CFD simulations are *Barrass*, *Millward*, *ICORELS* and *Hooft*. In the calculations, enforcement restrictions have been respected for all these methods.

In figure 6.13 the obtained results were compared with those validated in the literature and a very good resemblance is observed. *Jachowski* (2008) [19] compares CFD values with other empirical methods, but simulations were performed on a KCS model, for three depths and speeds ranging from 4 to 21.5 knots.

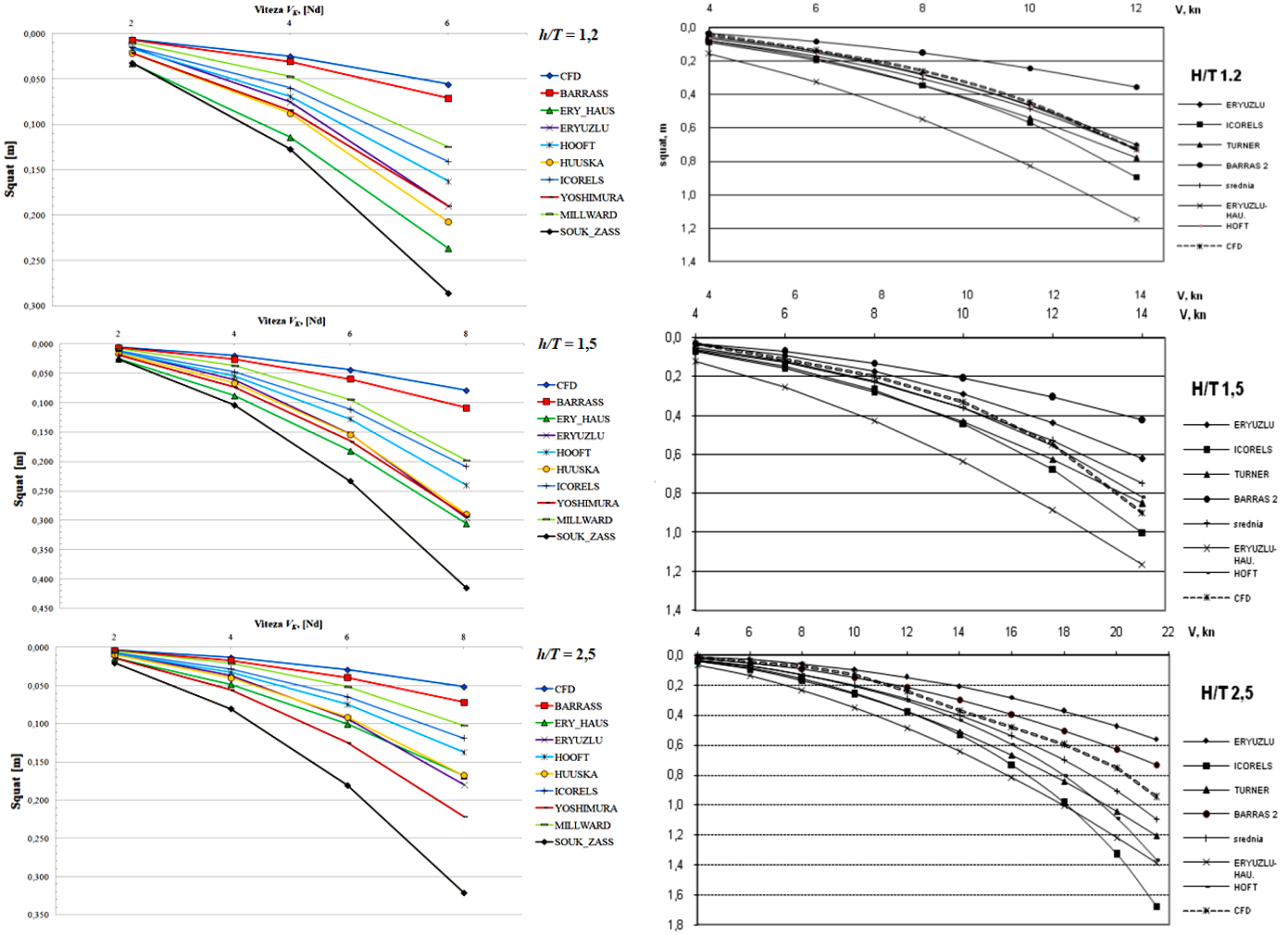

Fig. 6.13. Squat results comparison with literature for three *h/T* values [19]

The above comparisons show the influence of water depth and ship's speed on squat. It is noticed that squat calculated by the CFD method is consistent with most of the empirical methods presented, the *Barrass* method being the closest one to obtained values, overestimating with percentages between 12 % and 43 %, provided that all methods overestimate the squat, but with values exceeding 100 % to 500 %. Calculated squat values are between 0.0028 m and 0.078 m for real ship speeds of 2, 4, 6 and 8 knots.

The results of the study show that ANSYS CFX can be used effectively for the prediction of ship squat in shallow waters, but further investigation of hydrodynamic effects in confined channels is required.

CONCLUSIONS

C.1. GENERAL CONCLUSIONS

The research carried out within this thesis extends the problem of most accurate determination of ship squat, which is a very important aspect for the safety of navigation, especially in confined and shallow waters areas, where this phenomenon is more pronounced and has visible effects.

The main conclusions from the scientific research in the field of squat and its associated phenomena that occur when navigating through canals or shallow waters are:

- in the experimental studies conducted on scale models, it was observed that the most used model is KVLCC2, of a high-capacity tanker vessel, and for the achievement of conclusive results, the laboratory tests included a wide range of combinations between depth and width of the channel, as well as between depth and draft of the models used;
- the determination of squat depends on the characteristics of the ship and the configuration of the canal or waterway. The main parameters of the ship that influence the squat are the length, breadth, draft, block coefficient of fineness and speed. The aspects related to the parameters of the waterway are water depth, cross section of the channel and its width;
- the existence in the literature of numerous authors who have defined computational relations in order to estimate squat correctly, which have been modified and redefined for more than 50 years of research on the subject but have not yet reached a general form valid for all ship types and channel configurations;
- in the study case of squat on military ships in Sulina Canal, it was found that Frigate 1 and multirole support ship can cross the canal at a maximum speed of 8 knots, Frigate 2 with 12 knots, and the offshore patrol vessel with 16 knots. It has also been observed that the bow and stern drafts vary with speed and blockage factor according to *Barrass*'s formula. Another conclusion of the simulations is the observed difference between the desired speed, generated by the engine rotation and the actual speed over ground, which varied between 0.1 knots and 7 knots;
- in the analysis of the squat and under keel clearance for the most representative nine types of ships in the current naval industry, it was concluded that:
  - whatever the speed, ULCC ships cannot navigate through the rectangular or the trapezoidal canals, having the dimensions specified in the study, due to squat;
  - VLCC vessels can pass the rectangular canal with a speed up to 8 knots and the trapezoidal one with a speed up to 12 knots;
  - squat for other ship types falls within normal limits, and the under keel clearance is sufficient even at 12 knots, which allows transits of the considered canals.
- in the ship-to-ship interaction case study, there was observed an increase in the draft at the bow and stern of the ship, but also the occurrence of a pivoting moment that deviates the ship from the course. It has been concluded that a higher ship speed, a small distance between ships and a small under keel clearance provide a strong interaction between ships;
- studying the hydrodynamic parameters of a bulk carrier and ship-to-shore interaction using the NTPRO 5000 navigation simulator, it was concluded that the squat produced on the ship is greater in the approach to the canal's bank than in open waters. It has also been noted that the variation of the lateral force acting on the ship's body at the 7.4 knot speed has a similar trend for all studied depths. For the 16 knot speed, the bank effect is more pronounced and makes the ship's trajectory to be diverted to the opposite bank where the collision occurs;
- the following conclusions were drawn from the experimental research on board training ship "MIRCEA":
  - the only way on board to read the draft is through direct observation of the draft scales;
  - the geometric parameters of training ship "MIRCEA", such as length, breadth, draft or block coefficient of fineness, which are too small in comparison with the dimensions of the harbors, but also the low speed did not favor the occurrence of the squat in maneuvers of entry/exit to/from the ports of call;
  - the water depth in transit ports as well as the width of the navigable channel were variable, and the occurrence of squat was difficult to observe;

- as a result of numerical simulations, it has been observed that the fluid speed variation obtained in the fluid domain along the hull has a normal distribution with a potential increase in the flow rate below the hull due to the interaction between the ship's body and the bottom of the domain. Also, the pressure variation on hull is in accordance with the theoretical notions of a ship's pressure domain, with two positive pressure bulbs, one at the bow and one at the aft, and one at negative pressure zone at the bottom, along the hull;
- in order to evaluate the predictability of the squat prediction using the vertical hydrodynamic forces determined with ANSYS CFX, a comparison was made with nine of the most common empirical methods for the calculation of squat in shallow waters without lateral restrictions, and it was appreciated that the methods of *Barrass*, *Millward*, ICORELS and *Hooft* suit well with the values obtained by CFD simulations.

C.2. ORIGINAL CONTRIBUTIONS

Through the scientific research carried out and the obtained results, the following contributions were made:

a. theoretical contributions:
   - identification and description of the main navigable canals used in world shipping;
   - a presentation of the current state of research on the squat phenomenon, the evolution of research over time, the main ship models and towing tanks used in the experiments;
   - a comprehensive presentation of the empirical computational relations of the squat found in the literature, which identified the channel types where these relationships can be used and the restrictive application conditions;

b. numerical contributions:
   - performing a case study by simulation on squat occurrence at four military ships similar to those of the Romanian Naval Forces, when they navigate at different speeds at the entrance to the Sulina Canal;
   - the analysis of squat and under keel clearance for nine types of commercial ships, ranging from super tankers to tugs, which transits at 6, 8, 10 and 12 knots, two channel categories, one with a rectangular transverse section and a trapezoidal one;
   - calculation of a general cargo ship squat in channels of different widths and depths to observe the maximum squat variation at speed increase and determine the maximum speed at which the grounding occurs on the channel;
   - the conduction of a case study on the hydrodynamic interaction of two vessels in a canal – the meeting situation;
   - a case study on hydrodynamic interaction between a general cargo ship and the bank of a section of the Suez Canal;
   - calculation of squat by CFD method and analysis of its variation according to speed and depth of the fluid domain;
   - a comparative study between the squat determined by the hydrodynamic forces obtained with the ANSYS CFX and the squat calculated with 9 empirical relations existing in the literature, for the hull of training ship "MIRCEA";

c. experimental contributions:
   - elimination of the difficulty in reading stern draft on board training ship "MIRCEA" by recording it with a video camera and reading the draft values later;
   - an analysis of the speed, draft and trajectory of the ship at the entrance/exit to/from the ports of call of the international voyage;
   - geometrically modeling of the training ship "MIRCEA";
   - performing 22 CFD numerical simulations for observing the variation of hydrodynamic pressures, velocities and forces acting on the hull when moving at four speeds in a fluid domain of varying depths.

C.3. FUTURE DEVELOPMENT PERSPECTIVES

The steps taken during the elaboration of the PhD thesis allow the further development of the theoretical and experimental researches in the following directions:

- conducting numerical simulation research on the hydrodynamic effects produced on ship maneuvering in locks, in order to study the ship's flow domain and its interaction with the lock walls;
- building a scale model of the training ship "MIRCEA" hull and experimental analysis of the squat phenomenon when moving it into a shallow water towing tank;
- performing CFD numerical simulations on the production of squat at training ship "MIRCEA" hull under different conditions, such as: when moving in channels of variable widths and depths; adding the propeller and rudder to the hull geometry to determine their hydrodynamic influence from the point of view of squat production; defining the hull with 6 degrees of freedom and moving it into a free surface domain with dynamic mesh, to study the wave production in shallow water areas.

C.4. DISSEMINATION OF RESULTS

The results of theoretical and experimental researches on the subject obtained during the doctoral studies were capitalized by:

a. 11 scientific papers published:
   - one ISI Web of Knowledge indexed article (sole author);
   - 7 articles included in international databases (2 sole author, 5 first author);
   - 3 articles in the volumes of international and national scientific events (3 first author);

b. participation with scientific papers at 9 national and international conferences.

ACKNOWLEDGMENT

The work has been funded by the Sectorial Operational Programme Human Resources Development 2007-2013 of the Ministry of European Funds through the Financial Agreement POSDRU/159/1.5/S/132395.

SELECTIVE REFERENCES

[1] *Y. M. Ahmed*, "Numerical Simulation for the Free Surface Flow around a Complex Ship Hull Form at Different Froude numbers", in Alexandria Eng. Journal, **vol. 50**, no. 3, 2011, pp. 229-235.

[2] *N. Alderf, E. Lefrançois, P. Sergent and P. Debaillon*, "Transition Effects on Ship Sinkage in Highly Restricted Waterways", in Proceedings of the Institution of Mechanical Engineers, Part M: Journal of Engineering for the Maritime Environment, **vol. 224**, issue2, June 2010, pp. 141-153.

[3] *C. B. Barrass*, Ship Design and Perfomance for Masters and Mates, Editura Elsevier, Londra, 2007.

[4] *C. B. Barrass, D. R. Derrett*, Ship Stability for Masters and Mates, 7th ed., Editura Elsevier, Oxford, 2012.

[5] *A. Biran, R. Lopez-Pulido*, Ship Hydrostatics and Stability, 2nd ed., Editura Elsevier, Oxford, 2014.

[6] *M. J. Briggs*, "Ship Squat Predictions for Ship/Tow Simulator", in Coastal and Hydraulics Engineering Technical Note 72, US Army Engineer Research and Development Center, Vicksburg, 2006.

[7] *M. J. Briggs, P. J. Kopp, V. Ankudinov and A. L. Silver*, "Ship Squat Comparison and Validation using PIANC, Ankudinov and BNT Predictions", in The 2nd International Conference on Ship Manoeuvring in Shallow and Confined Water: Ship to Ship Interaction, Trondheim, May 2011, pp. 59-70.

[8] *M. J. Briggs, M. Vantorre, K. Uliczka and P. Debaillon*, "Prediction of Squat for Undeekeel Clearance", in Handbook of Coastal and Ocean Eng., Los Angeles, 2010, pp. 723-774.

[9] *Gina M. Casadei*, Dynamic-mesh Techniques for Unsteady Multiphase Surface-Ship Hydrodymanics, Master Thesis, The Pennsylvania State University, 2010.

[10] *P. Debaillon*, "Numerical Investigation to Predict Ship Squat", in Journal of Ship Research, **vol. 54**, no.2, June 2010, pp. 133-140.

[11] *G. Delefortrie, M. Vantorre, K. Eloot, J. Verwilligen and E. Lataire*, "Squat Prediction in Muddy Navigation Areas", in Ocean Eng., **vol. 37**, 2010, pp. 1464-1476.

[12] *K. Eloot, M. Vantorre*, Ship Behaviour in Shallow and Confined Water: an Overview of Hydrodinamic Effects through EFD, Editura Maritime Technology Division, Ghent, 2007.

[13] *K. Eloot, M. Vantorre et al.*, "Squat During Ship-to-Ship Interactions in Shallow Water", in The 2nd International Conference on Ship Manoeuvring in Shallow and Confined Water: Ship to Ship Interaction, Conference Proceedings, Royal Institution of Naval Architects, London, 2011, pp. 117-126.

[14] *K. Ellot, J. Verwilligen and M. Vantorre*, "An Overview of Squat Measurements for Container Ships in Restricted Water", in Safety and Operations in Canals and Waterways, Conference Proceedings, Glasgow, 2008, pp. 106-116.

[15] *T. Gourlay*, "A Brief History of Mathematical Ship-Squat Prediction, Focussing on the Contributions of E. O. Tuck", in Journal of Engineering Mathematics, **vol. 70**, issue 1-3, July 2011, pp. 5-16.

[16] *T. Gourlay*, "Sinkage and Trim of Two Ships Passing Each Other on Parallel Courses", in Ocean Eng., **vol. 36**, issue 14, Oct. 2009, pp. 1119-1127.

[17] *A. Iranzo, J. Domingo, I. Trej, M. Terceno and J. Valle*, "Calculation of the Resistance and the Wave Profile of a 3600 TEU Container Ship", in Congreso MARINE 2007, Barcelona, June 2007, pp. 1-6.

[18] *E. C. Gh Isbășoiu*, Tratat de mecanica fluidelor, Editura AGIR, București, 2011.

[19] *J. Jachowski*, "Assessment of Ship Squat in Shallow Water using CFD", in Archives of Civil and Mechanical Eng., **vol. VIII**, no. 1, 2008, pp. 27-36.

[20] *E. Lataire, M. Vantorre and G. Delefortrie*, "A Prediction Method for Squat in Restricted and Unrestricted Rectangular Fairways", in Ocean Eng., **vol. 55**, Dec. 2012, pp. 71-80.

[21] *E. Lataire, M. Vantorre, J. Vandenbroucke and K. Eloot*, "Ship to Ship Interaction Forces during Lightering Operations", in The 2nd International Conference on Ship Manoeuvring in Shallow and Confined Water: Ship to Ship Interaction, Conference Proceedings, Royal Institution of Naval Architects, London, 2011, pp. 211-222.

[22] *D. Obreja*, Teoria navei – Concepte și metode de analiză a peformanțelor de navigație, Editura Didactică și Pedagogică, București, 2005.

[23] *David Frisk and Linda Tegehall*, Prediction of High-Speed Planing Hull Resistance and Running Attitude – A Numerical Study Using Computational Fluid Dynamics, Master Thesis, Chalmers University of Technology, Göteborg, 2015.

[24] *P. Senthil and C. Bihod*, "Numerical Estimation of Shallow Water Resistance of a River-Sea Ship using CFD", in International Journal of Computer Applications, **vol. 71**, no. 5, 2013, pp. 33-40.

[25] *F. Stern et al.*, "Computational Ship Hydrodynamics: Nowadays and Way Forward", in International Shipbuilding Progress, **vol.60**, no. 1-4, 2013, pp. 3-105.

[26] *J. Verwilligen and J. Richter*, "Analysis of Full Ship Types in High-blockage Lock Configurations", in MARSIM 2012, Singapore, Dec. 2012, pp. 1-10.

[27] *H. Wang, Z. Zou*, "Numerical Prediction of Hydrodynamic Forces on a Ship Passing Through a Lock", in China Ocean Eng., **vol. 28**, no. 3, 2014, pp. 421-432.

[28] *J. Yao and Z. Zou*, "Calculation of Ship Squat in Restricted Waterways by Using a 3D Panel Method", in Journal of Hydrodynamics, ser. B, **vol. 22**, issue 5, supplement 1, Oct. 2010, pp. 489-494.
[29] *H. Yoon, C. D. Simonsen, L. Benedetti, J. Longo, Y. Toda and F. Stern*, "Benchmark CFD Validation Data for Surface Combatant 5415 in PMM Maneuvers – Part I : Force/moment/motion Measurements", in Ocean Eng., **vol. 109**, 2015, pp. 705–734.
[30] *H. Zeraatgar, K. Vakilabadi and R. Yousefnejad*, "Parametric Analysis of Ship Squat in Shallow Water by Model Test", in Brodo Gradnja, **vol. 62**, 2011, pp. 37-43.
[31] *W. Zhang, Z. J. Zou and D. D. Deng*, "A Study on Prediction of Ship Maneuvering in Regular Waves", in Ocean Eng., **vol. 137**, May 2017, pp. 367-381.
[32] *L. Zou and L. Larsson*, "Computational Fluid Dynamics (CFD) Prediction of Bank Effects including Verification and Validation", in Journal of Marine Science and Technology, **vol. 18**, issue 4, Dec. 2013, pp. 310-323.
[33] *L. Zou and L. Larsson*, "Confined Water Effects on the Viscous Flow around a Tanker with Propeller and Rudder", in International Shipbuilding Progress, **vol. 60**, 2013, pp. 309-343.
[34] *** Ansys Inc., ANSYS CFX 16.2 documentation, 2015.
[35] *** Technical documentation of sailing ship "MIRCEA"
[36] *** Proceedings of the 23rd ITTC – The Manoeuvring Committee (vol. 1), 2002.
[37] http://www.bankeffects.ugent.be
[38] http://www.pianc.org
[39] http://www.shallowwater.be
[40] http://www.suezcanal.gov.eg